UNIVERSITY OF CALIFORNIA,
IRVINE

Spatial Memory Networks in Aging and Alzheimer's Disease

DISSERTATION

submitted in partial satisfaction of the requirements
for the degree of

DOCTOR OF PHILOSOPHY

in Biological Sciences

by

Freddie Márquez

Dissertation Committee:
Professor Michael A. Yassa, Chair
Associate Professor John Guzowski
Professor Elizabeth Head

2021

DEDICATION

To Alfonso and Dolores Marquez.

To Monica and Agustin Segura.

To Alfonso Luis Marquez.

To Drs. Silliker, Stutzmann, Garcia-Añoveros, and Cantú.

TABLE OF CONTENTS

LIST OF FIGURES ..... **V**

LIST OF TABLES ..... **VI**

LIST OF ABBREVIATIONS ..... **VII**

ACKNOWLEDGEMENTS ..... **VIII**

CURRICULUM VITAE ..... **IX**

ABSTRACT OF THE DISSERTATION ..... **XIV**

CHAPTER 1: BACKGROUND AND SIGNIFICANCE **1**

1.1 Background and public health relevance 1
1.2 Biomarkers for Assessing Aging and Alzheimer's Disease 2
1.2.1 The current classification of Alzheimer's disease 2
1.2.2 Pathology and spatiotemporal spread 3
1.2.3 Biomarker-based staging of Alzheimer's disease 4
1.3 Memory systems and Episodic Memory 5
1.3.1 The role of the medial temporal lobe in episodic memory 5
1.3.2 Pattern separation in the hippocampus 7
1.3.3 Pattern separation and neurocognitive aging 8
1.3.4 Functional neocortical networks 10
1.3.5 Memory systems and PMAT networks 12
1.3.6 Mild cognitive Impairment and Alzheimer's Disease 13

CHAPTER 2: ESTABLISHING CONVERGENT VALIDITY OF SPATIAL PATTERN SEPARATION **14**

Introduction 14
Materials and Methods 15
Results 16
Discussion 21

CHAPTER 3: SPATIAL PATTERN SEPARATION AND PMAT FRAMEWORK **23**

Introduction 23

MATERIALS AND METHODS 23
RESULTS 26
DISCUSSION 28

CHAPTER 4: SPATIAL PATTERN SEPARATION AND ALZHEIMER'S DISEASE PATHOLOGY 29

INTRODUCTION 29
MATERIALS AND METHODS 30
RESULTS 31
DISCUSSION 36

CHAPTER 5: SPATIAL PATTERN SEPARATION AND COGNITIVE DECLINE 38

INTRODUCTION 38
MATERIALS AND METHODS 38
RESULTS 39
DISCUSSION 41

CHAPTER 6: SYNTHESIS AND FUTURE DIRECTIONS 41

GENERAL SUMMARY 41
FUTURE DIRECTIONS 44

REFERENCES 48

APPENDIX A 75

LIST OF FIGURES

CHAPTER 1

Figure 1. Projected number of people with AD in the US population, 2020 to 2060.....2
Figure 2. MTL circuits involved in episodic memory 7

CHAPTER 2

Figure 3. Spatial lure discrimination is associated with RAVLT delayed recall 19
Figure 4. Spatial lure discrimination is associated with Retroactive Interference 20

CHAPTER 3

Figure 5. Functional connectivity of the posteromedial system associated with Spatial Lure Discrimination Index.....27

CHAPTER 4

Figure 6. Relationship between CSF biomarkers, spatial lure discrimination index (LDI), and RAVLT delayed recall 33
Figure 7. CSF biomarker group differences in functional connectivity.....35

CHAPTER 1

Figure 8. Spatial discrimination predicts annualized percent change of MMSE 40

APPENDIX A

Figure A1. CSF biomarkers are highly correlated with Aβ-PET in cognitively normal older adults 81
Figure A2. Positivity on Aβ-PET and CSF biomarkers are highly concordant in cognitively normal older adults.....83
Figure A3. Recalculation of thresholds for CSF Aβ42/40 and p-tau/A42 in a cognitively normal sample 85

LIST OF TABLES

CHAPTER 2

Table 1. Demographics and neuropsychological test scores 18

APPENDIX A

Table A1. Demographics and summary measures of the cognitively normal older adult cohort. 78

LIST OF ABBREVIATIONS

Aβ Beta-Amyloid

ACC Anterior Cingulate Cortex

AD Alzheimer's disease

ADRC Alzheimer's Disease Research Center

AFNI Analysis of Functional NeuroImages

CIND Cognitively Impaired Non-Demented

CDR Clinical Dementia Rating Scale

DG Dentate gyrus

EC Entorhinal cortex

MCI Mild cognitive impairment

MMSE Mini-Mental State Exam

MPFC Medial Prefrontal Cortex

MPRAGE Magnetization-Prepared Rapid Acquisition Gradient Echo MRI Magnetic resonance imaging

MTL Medial temporal lobe

PCC Posterior Cingulate Cortex

PHC Parahippocampal cortex

POR Postrhinal cortex

PRC Perirhinal cortex

RAVLT Rey Auditory Verbal Learning Test

ROI Region of Interest

RSC Retrosplenial

ACKNOWLEDGEMENTS

I sincerely thank my advisor, mentor, and the chair of my doctoral committee, Dr. Michael Yassa. His support throughout the years has been instrumental to my professional growth, and my training as a scientist. His optimism, and willingness to support my ideas have always been encouraging.

I also want to thank the past and present members of my committee, Drs. John Guzowski, Elizabeth Head, Claudia Kawas, Mark Mapstone, Jorge Busciglio, and Daniel Gillen. I appreciate their feedback and support. It has pushed me to think critically and has helped me move forward.

I thank the Yassa Lab for providing the intellectual environment that has allowed me to flourish. I have been surrounded by brilliant and kind people that have made this a delightful experience. I thank Maria Montchal for her mentorship, and Liv McMillan for her leadership. I thank the many people that have made this all possible including Myra S. Larson, Blake Miranda, Jenna Adams, Logan Harriger, and Jessica Noche. I thank the other members of the lab including Jared Roberts, Natalie DiProspero, Miranda Chappel-Farley, Sarah Kark, Soyun Kim, Batool Rizvi, Joren Adams, Anna Smith, Luis Colon-Perez, Caroline Chwiesko, Zachariah Reagh, John Janecek, Sandra Gattas, Steven Granger, Rebecca Stevenson, Jessica Yaros, Mithra Sathishkumar, Martina Hollearn and the past and present research assistants for their contributions and lunch conversations as well.

I also thank Manuella Yassa for her leadership, the Center for the Neurobiology of Learning and Memory (CNLM) and the CNLM ambassadors. I thank Allison Haskell for her mentorship, and friendship. I thank Maria Torres, Elizabeth Spangenberg, Elena Dominguez, Isabella Sanchez, and Miguel Arreola for their friendship, and conversations. I thank Dr. Jorge Cantú for his mentorship, friendship, and support throughout the years.

The work in this dissertation has been financially supported by US NIH grant R01AG053555 (PI: M.A.Y.) as well as the generous grants from the Alzheimer's Disease Research Center at UCI and the UC Institute for Memory Impairments and Neurodegenerative Disorders (UCI MIND). I also thank the National Science Foundation Graduate Research Fellowship Program and Bridge to the Doctorate, and the Department of Veterans Affairs Post 9/11 GI Bill. I am also grateful for the support from the Kavli Summer Institute in Cognitive Neuroscience, and the friends of the CNLM who have contributed to the Jared M. Roberts Memorial Graduate Student Award and the Pedagogical Fellowship for Brain Camp at UCI.

CURRICULUM VITAE

Education

Biological Sciences, **Bachelor of Science degree (B.S.)** 2010 – 2013
DePaul University; Chicago, IL

Neurobiology & Behavior, **Master of Science degree (M.S.)** 2015 – 2019
University of California Irvine; Irvine, CA

Neurobiology & Behavior, **Ph.D. Candidate** 2019 – Present
University of California Irvine; Irvine, CA

Experience

Cryptologic Technician (Naval Intelligence) 2006 – 2010
Navy Information Operations Command (NIOC); Yokosuka, Japan
United States Navy

Undergraduate Research Assistant 2012
Neuroscience Department
Rosalind Franklin University; North Chicago, IL
Principal Investigator: Grace Stutzmann, Ph.D.

Undergraduate Research Assistant 2012 – 2013
Biological Sciences Department
DePaul University; Chicago, IL
Principal Investigator: Margaret Silliker, Ph.D.

Research Technician 2014 – 2015
Sensory and Developmental Neurobiology Laboratory
Anesthesiology Department
Northwestern University; Chicago, IL
Principal Investigator: Jaime Garcia-Añoveros, Ph.D.

Graduate Research Fellow 2016 – Present
Translational Neuroscience Laboratory
Department of Neurobiology & Behavior
University of California, Irvine
Principal Investigator: Michael A. Yassa, Ph.D.

Awards and Honors

DePaul/Rosalind Franklin University Summer Research Program 2012

Louis Stokes Alliance for Minority Participation Award 2012 – 2013
National Science Foundation

Bridge to the Doctorate Award - National Science Foundation 2015 – 2017
($30,000/year stipend and $10,500/year tuition and fees for 2 years)

Eugene Cota-Robles Fellowship – UC Irvine Graduate Division 2017 – 2019

Graduate Research Fellowship - National Science Foundation 2017 – 2020
($34,000/year stipend and $12,000/year tuition and fees for 3 years)

Kavli Summer Institute in Cognitive Neuroscience Fellowship 2017
(Tuition, course materials, meals, and hotel)

Kavli Summer Institute in Cognitive Neuroscience Fellowship 2018
(Tuition, course materials, meals, and hotel)

Jared M. Roberts Memorial Graduate Student Award 2018
Center for the Neurobiology of Learning and Memory

Pedagogical fellowship Brain Camp at UCI 2019
Center for the Neurobiology of Learning and Memory

Science Communication

Courses/Workshops

Activate to Captivate Workshop with Bri McWhorter 2015

Neuroblitz – Department of Neurobiology and Behavior 2016 – Present
(one 15 minute research presentation per year)

Graduate Professional Success in Biomedical Sciences (GPS-BIOMED) 2016 – 2018
Science Policy Workshops

Science Communication Skills with Sandra Tsing Loh (BIO 270) 2019

Outreach

Science Fair Judge – Irvine Unified School District 2016

Research and Education in Memory Impairments and 2016 – 2017
Neurological Disorders (REMIND)

Center for the Neurobiology of Learning and 2017 – Present
Memory (CNLM) Ambassadors

Professional Activities and Memberships

Memberships

Member, Society for the Advancement of Chicanos, Native Americans in Science
Member, Society for Neuroscience
Member, Center for the Neurobiology of Learning and Memory Ambassador

Conference Program Committees

Co-Chair 2016
REMIND Emerging Scientists Symposium at UCI
Abstract Reviewer 2018
LEARNMEM 2018, Huntington Beach, CA, USA

Initiatives

Member, End Racism Initiative 2021
(working group to increase recruitment of Black Faculty)
Department of Biological Sciences at UCI

Teaching Activities

Neurobiology and Behavior Laboratory – 20 Students, 25%	SQ 2018
Neurobiology and Behavior Laboratory – 20 Students, 25%	WQ 2018
Mind, Memory, Amnesia, and the Brain – 95 Students, 25%	SQ 2019
UCI Brain Camp	SU 2019
Sex Influences and the Brain – 53 Students, 25%	SQ 2020

Mentorship and Advising

Ali Ozgur 2016 – 2017
Undergraduate Student, Neuroscience, UC Irvine
Now graduate student at UC Irvine (Interdepartmental Neuroscience Program)

Myra Saraí Larson 2017 – 2019
Research Specialist, Department of Neurobiology and Behavior, UC Irvine
Now graduate student at UC Los Angeles

Blake Miranda 2018 – 2021
Research Specialist, Department of Neurobiology and Behavior, UC Irvine
Now graduate student at UC Los Angeles

Presentations

Marquez, F., Schneider, C., and Stutzmann, G. The effect of dantrolene treatment on synapse preservation in Alzheimer's disease mice. DePaul University's Natural Sciences, Mathematics and Technology Showcase. Chicago, IL. November 9, 2012.

Marquez, F., Francis, M., Silliker, M. RNA editing in *Didymium iridis* mitochondrial genes. Chicago Area Undergraduate Research Symposium. April 6, 2013.

Marquez, F., Noche, J., Larson, M.S., McMillan, L., Tustison, N., Delisle, D., Murray, E.A., Witbracht, M., Sirivong, S., Grill, J., and Yassa, M. A. Spatial discrimination performance predicts integrity of hippocampal cingulum in older adults. Society for Neuroscience. November 7, 2018.

Marquez, F., and Yassa, M. A. Spatial discrimination performance predicts integrity of hippocampal cingulum in older adults. Park City Learning and Memory Conference. January, 2019.

Marquez, F., Larson, M.S., Noche, J., McMillan, L., Tustison, N., Delisle, D., Murray, E.A., Witbracht, M., Sirivong, S., Grill, J., and Yassa, M. A. Functional connectivity of the medial temporal lobe contributes to spatial discrimination impairments in non-demented older adults. Society for Neuroscience. October 21, 2019.

Marquez, F., Larson, M.S., Smith, A., Miranda, B., Sathishkumar, M., McMillan, L., and Yassa, M. A. Neurocognitive mechanisms of spatial pattern separation in older adults with and without subclinical memory impairment. Research and Education in Memory Impairments and Neurological Disorders (REMIND) Emerging Scientists Symposium. February 21, 2020.

Marquez, F., Larson, M.S., Smith, A., Miranda, B., Sathishkumar, M., McMillan, L., and Yassa, M. A. Neurocognitive mechanisms of spatial pattern separation in older adults with and without subclinical memory impairment. Alzheimer's Association International Conference. July 15, 2020.

Publications

Journal Articles

Flores, E. N., Duggan, A., Madathany, T., Hogan, A.K., **Márquez, F.,** Kumar, G., Seal, R., Edwards, R, Liberman, M.C., García-Añoveros, J. (2015) A Non-Canonical Pathway for Auditory Nociception. *Current Biology*. https://doi.org/10.1016/j.cub.2015.01.009.

Wiwatpanit, T., Lorenzen, S. M., Cantú, J. A., Foo, C. Z., Hogan, A. K., **Márquez, F**., et al. (2018). Trans-differentiation of outer hair cells into inner hair cells in the absence of INSM1. *Nature*.

Márquez, F., and Yassa, M.A. Neuroimaging Biomarkers for Alzheimer's Disease. *Molecular Neurodegeneration* 2019; *14*, 21. doi: https://doi.org/10.1186/s13024-019-0325-5

Holbrook, AJ, Tustison, NJ, **Márquez, F.**, et al. Anterolateral entorhinal cortex thickness as a new biomarker for early detection of Alzheimer's disease. *Alzheimer's Dement*. 2020; 12:e12068. https://doi.org/10.1002/dad2.12068

Márquez, F., Noche, J.A., Harriger, L., Larson, M.S., Miranda, B., Smith, A., Hollearn, M., McMillan, L., Rissman, R. A., Head, E., and Yassa, M.A. Spatial pattern separation is linked to posteromedial network functional connectivity, Alzheimer's pathology, and cognitive decline in older adults. (submitted).

Márquez, F., Adams, J. N., Larson, M. S., Janecek, J.T., Miranda, B., Noche, J.A., Taylor, L., Hollearn, M., McMillan, Keator, D. B., Rissman, R., L., Head, E., and Yassa, M.A. CSF biomarkers of Alzheimer's pathology are highly concordant with amyloid-PET in cognitively normal older adults.

Book Chapters

Ashburn, S., Abugaber, D., Antony, J., Bennion, K., Bridwell, D., Cardenas-Iniguez, C., Doss, M., Fernández, L., Huijsmans, I., Krisst, L., Lapate, R., Layher, E., Leong, J., Li, Y., **Márquez, F.**, Munoz-Rubke, F., Musz, L., Patterson, T., Powers, J., Proklova, D., Rapuano, K., Robinson, S., Ross, J., Samaha, J., Sazma, M., Stewart, A., Stickel, A., Stolk, A., Vilgis, V., Zirnstein, M. Towards a socially responsible, transparent, and reproducible cognitive neuroscience. In M. Gazzaniga & R. Mangun, The Cognitive Neurosciences VI. Cambridge, MA: MIT Press.

ABSTRACT OF THE DISSERTATION

Spatial memory networks in aging and Alzheimer's disease

By

Freddie Márquez

Doctor of Philosophy in Biological Sciences

University of California, Irvine, 2021

Professor Michael A. Yassa, Chair

An estimated 6.1 million Americans currently suffer with Alzheimer's disease (AD) and in the absence of effective treatment or a cure, this number could increase to 13.8 million by 2060. One of the most common changes that occurs in aging and Alzheimer's disease is decline in memory for everyday experiences (episodic memory). Computational models suggest that the brain uses a neural computation known as *pattern separation* to distinguish among highly similar inputs during memory recall. Furthermore, episodic memory has several components: *what* happened, *where* it happened, and *when* it happened. The posteromedial cortices are regions that are thought to be involved in spatial memory and are early sites that are affected by AD pathology. Neuropathological hallmarks of AD include the presence of beta-amyloid (Aβ) plaques, and the formation of neurofibrillary tangles (NFT) and neuropil threads. Eventually, this is followed by neurodegeneration. *In vivo* candidate biomarkers for AD include pathological aggregations of misfolded proteins (e.g. amyloid plaques, [Aβ], and hyperphosphorylated tau tangles, as measured by CSF assays, and PET imaging), neuronal dysfunction or atrophy (as measured by functional or structural MRI, and total tau levels as measured by CSF assays), and cognitive impairment (as measured by neuropsychological tests). However, the relationship between the

pathological, neuroimaging, behavioral, and cognitive markers in the aging brain and in AD remains unclear. The goal of this dissertation was to understand how regions of the brain that support memory for where events occur (spatial memory) are altered in the context of Alzheimer's disease. We gave participants a spatial pattern separation task, in which we showed participants a series of objects on different locations on a screen and tested participants on their ability to remember the spatial location of the objects after a delay. We found that cortical regions known as the posteromedial network may support spatial pattern separation. Spatial pattern separation task performance was associated with word list delayed recall test commonly used in a clinical setting, a relationship that is conditional upon the level of amyloid burden. Spatial pattern separation task performance was also associated with AD pathology, and cognitive decline. These findings suggest that the pattern separation framework may provide an account for understanding mechanistic changes that occur in the progression of AD. Future studies of spatial memory should investigate associations between regionally specific effects of AD pathology, vascular and immune contributions to AD, and include community-based samples of ethnically diverse populations.

CHAPTER 1: Background and Significance

1.1 Background and public health relevance

Alzheimer's disease (AD) is the most common age-related dementia, with prevalence continuing to increase (Alzheimer's disease facts and figures, 2020). With the exception of AD cases caused by genetic mutations (i.e. familial AD), age is the greatest risk factor. Currently, one in ten people 65 years of age or older have AD. In addition, the average life expectancy of a person in the United States has increased by 9 years and the population of people 65 years of age and above has increased by 34 million people (16 million to 50 million) over the last 60 years. Today, an estimated 6.1 million Americans are living with AD and in the absence of effective treatment or a cure, this number could increase to 13.8 million by 2060 (Alzheimer's disease facts and figures, 2020). Thus, a critical goal of biomedical research is to establish indicators (i.e. biomarkers) of AD during the preclinical stage allowing for early diagnosis and intervention. Understanding the neurobiological processes that support memory could help find links between age-related and AD-related changes in the brain and the cognitive changes observed.

A critical goal of biomedical research is to establish cognitive and biological indicators of AD during preclinical and prodromal stages allowing for early diagnosis and intervention (Öhman et al., 2021). Biomarkers quantify characteristics of biological processes that can be linked to cognitive and clinical endpoints, thus can be used as surrogates of the disease process. Computerized cognitive assessments can serve as "digital biomarkers" by probing subtle features of cognitive decline during the earliest stages of the disease and can be linked with mechanistic biomarkers in a comprehensive approach to improve the efficiency of clinical trials (Papp et al., 2021).

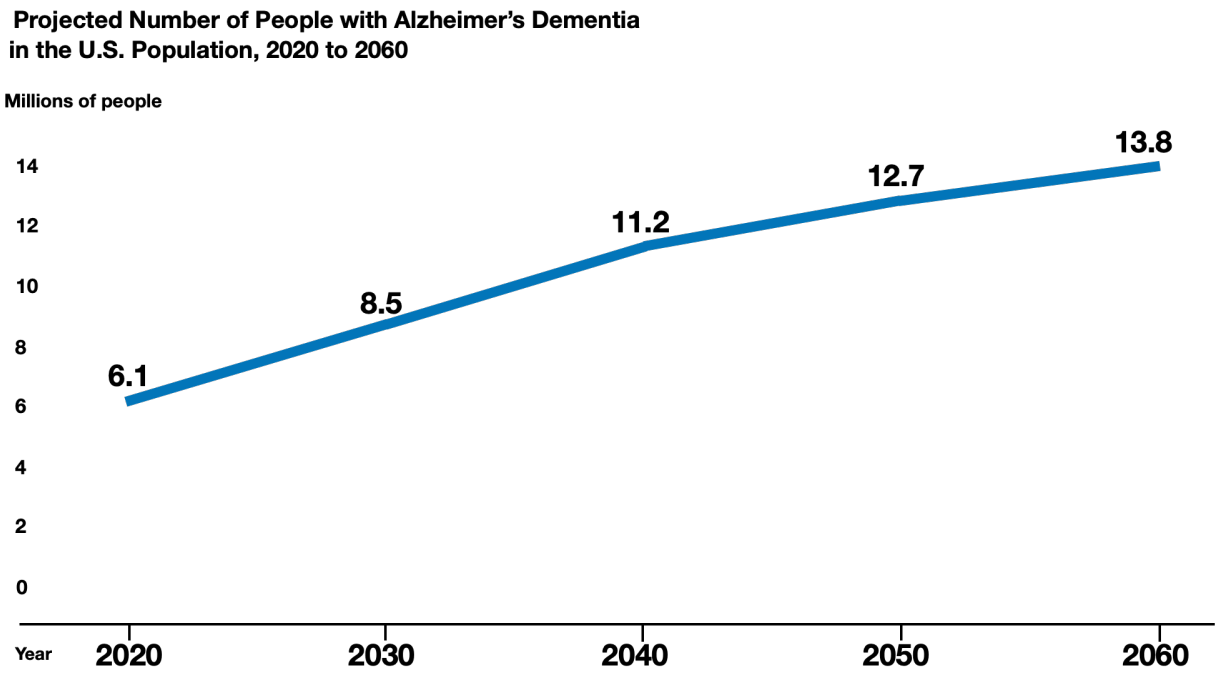

Figure 1. Projected number of people with AD in the US population, 2020 to 2060

1.2 Biomarkers for Assessing Aging and Alzheimer's Disease

1.2.1 The current classification of Alzheimer's disease

Identification of pathologic processes prior to the onset of disease symptoms is of critical importance to the field. Biomarkers are quantifiable characteristics of biological processes related to Alzheimer's disease that are linked to clinical endpoints and thus can be used as surrogates for the disease process. Historically, AD has been viewed as a disease of clinical symptoms in the clinical setting. By classifying AD in this manner, its diagnosis would likely include a considerable amount of non-AD cases as defined by its pathological characteristics. In 2011, the National Institute on Aging and the Alzheimer's Association (NIA-AA) Working Group put forth staging criteria that incorporate neuroimaging biomarkers (Sperling et al., 2011). The authors presented a conceptual framework and operational research criteria for preclinical AD where Stage 1 is characterized by the presence of asymptomatic β-amyloidosis, or increased

amyloid burden. Stage 2 includes neuronal injury and evidence of neurodegenerative change. Lastly, stage 3 additionally includes evidence of subtle cognitive decline, which is not yet sufficient for clinical diagnosis. The new research framework proposed by the NIA-AA defines AD pathologically with the use of biomarkers, which could potentially differentiate cases that clinically resemble AD such as hippocampal sclerosis. This framework additionally allows for staging using either fluid or neuroimaging biomarkers. However, certain features, which may be critical for the pathophysiology of the disease, could only be detected using imaging techniques. Hippocampal hyperactivity on task-activated functional MRI is one such example. Ewers et al. (Ewers et al., 2011) and Leal and Yassa (Leal and Yassa, 2013) include this feature in staging the disease and highlight that it seems to appear within a temporally constrained window. Jack and Holtzman (Jack and Holtzman, 2013) proposed several time-dependent models of AD that take into consideration varying age of onset as well as co-morbid pathologies.

1.2.2 Pathology and spatiotemporal spread

Neuropathological staging criteria of AD-related changes originally indicated that although the distribution of beta-amyloid (Aβ) neuritic plaques varies widely, neurofibrillary tangles and neuropil threads show a distribution pattern that allow for the differentiation of six stages (Braak and Braak, 1991). Stages I-II show alterations that are confined to the transentorhinal region, which spread to limbic (Stage III-IV), and finally to isocortical regions (Stage V-VI). More recently, pathology studies have indicated that intraneuronal aggregations of the protein tau seem to precede the extracellular deposition of Aβ by approximately a decade (Braak and Del Tredici, 2011; Duyckaerts and Hauw, 1997). Notably, non-argyrophillic tau lesions are thought to first appear in the locus coeruleus prior to the appearance of argyrophillic tau lesions caused by neurofibrillary tangles (NFTs) within the transentorhinal region of the cerebral cortex (Braak and

Tredici, 2015). Intraneuronal inclusions consisting of aggregated protein tau appear in selectively vulnerable cell types that appear to spread in a regionally and temporally specific manner that is independent of proximity to affected area (Braak and Braak, 1999). One advantage of using brain imaging techniques is that they operate at a higher level of spatiotemporal sensitivity than fluid biomarkers, thereby offering an opportunity to stage progression of the disease. Thus far, imaging using combinations of in vivo tau-PET and MRI techniques have shown progression patterns that largely recapitulate staging based on post-mortem histology (Schöll et al., 2015).

1.2.3 Biomarker-based staging of Alzheimer's disease

Out of the five biomarkers proposed by the NIA-AA, three were imaging biomarkers (amyloid PET, structural MRI, and FDG PET). Anatomical information from imaging biomarkers may provide crucial disease-staging information. This would imply an advantage for imaging biomarkers over fluid biomarkers because imaging can distinguish the different phases of the disease both temporally and anatomically. However, in recent years, assays to measure CSF biomarkers have been developed for measurement on high-throughput automated platforms, including the Fujirebio Lumipulse assay, resulting in a more consistent analytical process. Few studies have assessed the agreement of amyloid PET and CSF biomarkers on Lumipulse. Consistent with other studies, our data show that when comparing amyloid-PET and composite CSF measures of Aβ, 18F-Florbetapir was highly correlated with Aβ42/40 ($r = -0.810$, $p < 0.0001$), and p-tau/Aβ42 ($\rho = -0.841$, $p < 0.0001$) (**APPENDIX A**). Additionally, using pre-established cutoffs that were defined based on receiver operating characteristic analysis of amyloid PET and the CSF measures, classification performance was high between 18F-

Florbetapir and composite measures of Aβ such as p-tau/Aβ42 (AUC = 0.95), and Aβ42/40 (AUC = 0.92) (**APPENDIX A**).

The NIA-AA research framework has more recently been updated (Jack et al., 2018; Jack Jr et al., 2013) to focus on A/T/N criteria, first proposed by Jack and colleagues (Jack et al., 2016) and pave the path to more personalized diagnosis and treatment. The new framework highlights the value of positive amyloid biomarkers (A) to specifically indicate AD-related processes. Pathological tau (T) is only taken to indicate an AD-related process in the presence of amyloid positivity. Finally, (N) biomarkers are thought to provide nonspecific information about neuronal injury and neurodegenerative change. The combination of amyloid with other biomarkers can then be used to stage AD progression. Additionally, according to this new framework, the presence of tau and neurodegeneration in the absence of amyloidosis is considered evidence for non-AD pathological processes. An important aspect of the 2018 NIA-AA working group framework is the flexibility to include additional biomarkers in future iterations. We recently reviewed established and emerging neuroimaging biomarkers for Alzheimer's disease (Márquez and Yassa, 2019).

1.3 Memory systems and Episodic Memory

1.3.1 The role of the medial temporal lobe in episodic memory

The medial temporal lobe contains a set of structures that play an important role in declarative long-term memory (facts and events) processing, which is severely impacted in amnestic forms of AD. It consists of the hippocampal formation (HF: CA1-4, dentate gyrus – DG, subiculum, presubiculum, parasubiculum), perirhinal (PRC), entorhinal (EC), and

parahippocampal/postrhinal (PHC/POR) cortices. These structures are highly interconnected and support distinct information processing streams (Ranganath and Ritchey, 2012). The lateral (LEC) contains neurons and circuits representing information about objects and their complexity, object traces over time, and sequences of an event (parameters that represent the specific content and temporal order of an event (Deshmukh and Knierim, 2011; Montchal et al., 2019; Reagh and Yassa, 2014; Rodo et al., 2017; Tsao et al., 2013, 2018; Van Cauter et al., 2013; Wang et al., 2018; Wilson et al., 2013a, 2013b). In contrast, studies in animals and in humans indicate that the medial EC (MEC) stream contains a high percentage of spatially modulated neurons such as grid, head direction, border, aperiodic spatial and object-vector cells (parameters necessary for spatial navigation) (Doeller et al., 2010a; Hafting et al., 2005; Høydal et al., 2019; Jacobs et al., 2013; Killian et al., 2012; Miao et al., 2017; Sargolini et al., 2006; Solstad et al., 2008). Neuroanatomical and neuroimaging studies have indicated that the PHC (homologous to the POR in rodents) carries visuospatial/contextual information ('where' stream) to the MEC, and the PER carries item/object information to the LEC ('what' stream) (Burwell and Amaral, 1998; Maass et al., 2015; Naber et al., 1997; Navarro Schröder et al., 2015; Schultz et al., 2015; Suzuki and Amaral, 1994). These two streams converge in the HF, where they are combined and further processed to construct a complete memory representation (Eichenbaum et al., 2007; Ranganath and Ritchey, 2012; Yassa and Stark, 2011; Yonelinas and Ritchey, 2015).

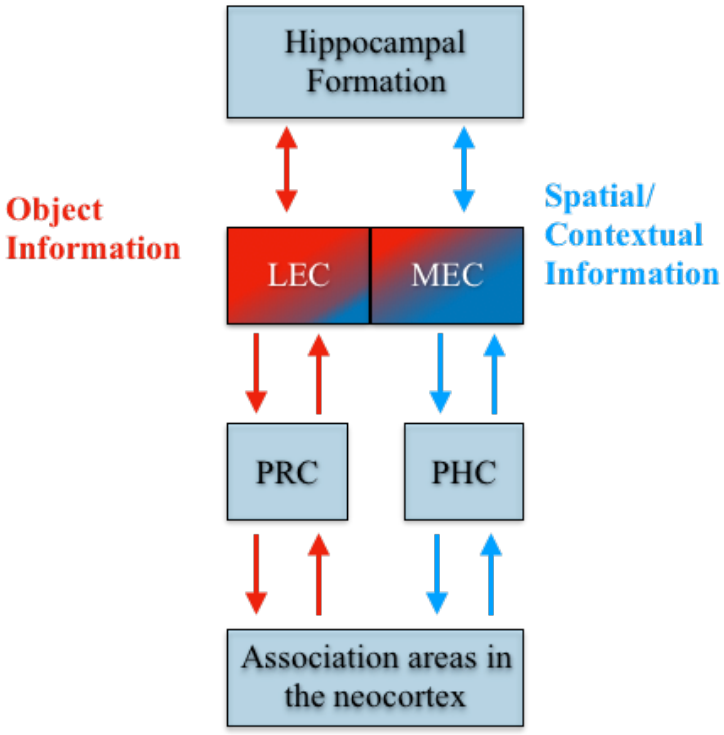

Figure 2. MTL circuits involved in episodic memory

1.3.2 Pattern separation in the hippocampus

Episodic memory is often defined as records of unique experiences and events that guide adaptive behavior; a feature of the brain that is thought to be reliant on the hippocampus (Milner et al., 1998; Squire et al., 2004). A key feature of episodic memory is the ability to discriminate among highly similar experiences thus creating dissociable experiences from one day to the next. Computational models suggest that the brain uses a neural computation known as *pattern separation* to distinguish among highly similar items during memory performance (Marr, 1971). This computation is thought to be heavily reliant on the dentate gyrus (DG) and CA3 of the hippocampus and serves to create orthogonalized representations from similar inputs (Yassa and Stark, 2011). More specifically, the DG is thought to be capable of pattern separation while the

CA3 region acts in an auto-associative network capable of both pattern separation as well as *pattern completion* via its recurrent collateral network**.** Pattern completion in this sense, refers to the process by which incomplete representations are "filled in" based on previously stored information (Yassa and Stark, 2011).

1.3.3 Pattern separation and neurocognitive aging

Through the advances made in neurocognitive aging studies, it is now possible to develop and validate behavioral paradigms that can dissociate and provide information about the functional integrity of underlying systems. The hippocampal dentate gyrus (DG)/CA3 network is hypothesized to engage in minimization of interference among overlapping memories, i.e. pattern separation (Yassa and Stark, 2011). This capacity is diminished in aged rats with memory impairment (Wilson et al., 2006). Using high-resolution functional MRI, object discrimination performance is linked to functional rigidity, or the inability to pattern separate unless interference is minimal, as well as hyperactivity in the DG/CA3 region in older adults (Yassa et al., 2011a, 2011b). The hyperactivity reported is consistent with other studies of hippocampal memory in MCI patients (Dickerson et al., 2004, 2005; Miller et al., 2008a) and in older adults *with* subclinical memory impairments (defined by the RAVLT Delay) (Miller et al., 2008b; Yassa et al., 2010). Other work has also shown that increased hippocampal activity negatively correlates with thinning in several regions, including the entorhinal cortex (EC) (Putcha et al., 2011). This work has recently been extended beyond object discrimination to show that aging is associated with impaired spatial (Reagh et al., 2014) and temporal (Roberts et al., 2014) discrimination.

Using a task concurrently taxing object versus spatial mnemonic discrimination, thought to tax pattern separation (orthogonalization of similar inputs into dissimilar outputs) in the

hippocampus, shows that while older adults *without* subclinical memory impairments (defined by the RAVLT Delay) have major deficits on object discrimination, they only show subtle deficits on the comparable spatial discrimination task when compared to young adults (Reagh et al., 2016). Recent human fMRI studies have identified a functional dissociation within the EC, with anterolateral (aLEC) and posteriomedial (pMEC) subregions similar to what is found in rodents (Maass et al., 2015). In the task-activated fMRI version of the object versus spatial task, the results show domain-general hippocampal engagement, but selective engagement of PRC and LEC during object discrimination and engagement of PHC and MEC during spatial discrimination (Reagh and Yassa, 2014). Furthermore, engagement of the DG/CA3 and aLEC correlate with performance on the object discrimination task to reveal an imbalance of the DG/CA3-aLEC circuit (hyperactivity of DG/CA3 and hypoactivity of the aLEC) in the absence of structural thinning of the regions in healthy older adults (Reagh et al., 2018).

Although it is presently unclear whether dysfunction in these brain regions is exclusive to pathological aging, or is also a feature of healthy aging, much evidence suggests that the PRC and LEC are among the earliest areas affected (Reagh et al., 2018). As PRC and LEC project to the hippocampus, it is likely that disruptions in these input regions also disrupt hippocampal computations during object discrimination, but less so during spatial discrimination. Conversely, other neighboring cortices thought to process spatial or contextual information (such as PHC and MEC) may be relatively spared in the absence of age-related neuropathology. Older adults *with* subclinical memory impairments (defined by the RAVLT Delay) show impaired performance on both aspects of the task, which suggests that both the item/object and context/spatial neural circuits may be negatively impacted. Studies evaluating mnemonic discrimination of spatial information were based on early work in hippocampal-lesioned rodents (Gilbert et al., 1998),

which assessed the ability to judge whether stimuli had moved from locations in which they were originally presented. The difficulty of discrimination is typically tested by systematically varying the metric distance between the study and test phases. Recent studies have used spatial mnemonic discrimination tasks and have found that a subset of older adults who were impaired (based on the RAVLT) were significantly impaired on the spatial discrimination task compared to unimpaired older adults and young adult groups (Reagh et al., 2014; Stark et al., 2010). Another study (Holden and Gilbert, 2012), using a delayed-match-to-sample discrimination task also showed impairments in the ability for older adults to discriminate spatial information.

1.3.4 Functional neocortical networks

Functional MRI techniques are based on blood-oxygenation-level-dependent (BOLD) contrast, which is associated with neural activity at the population level. Resting-state functional magnetic resonance imaging (rsfMRI) studies examine the temporal correlation of the BOLD signal between the regions of interest (or functional connectivity) by analyzing task-independent spontaneous fluctuations in brain networks (Biswal et al., 1995; Fox and Raichle, 2007). An emerging systems-based model of AD considers the large-scale disruptions across the course of AD. In preclinical AD, studies have generally noted that resting state fMRI (rsfMRI) is linked to metabolic changes (indexed by PET imaging) and precedes neurodegeneration (review by Sheline and Raichle, 2013). Most analyses have focused on the default mode network (DMN) (Gusnard and Raichle, 2001; Raichle et al., 2001) - a network that involves the medial prefrontal cortex, posterior cingulate cortex, precuneus, anterior cingulate cortex, parietal cortex, and the medial temporal lobe, including the hippocampus (Buckner et al., 2008; Greicius and Menon, 2004). As regions within the DMN are highly overlapping with the spatial distribution of both

amyloid and tau pathology (Buckner et al., 2008), resting state fMRI can offer important information on the integrity of these circuits and the degree to which their synaptic connectivity may be affected by the disease process. While some studies have found that alterations to DMN connectivity become more dramatic with disease progression, others have found dynamic changes that relate to Aβ and tau-specific profiles (Jones et al., 2016; Petrella et al., 2011; Sanz-Arigita et al., 2010; Schultz et al., 2017; Sepulcre et al., 2016; Supekar et al., 2008; Zhang et al., 2010). Connectivity changes in other networks have also been reported (Fredericks et al., 2018). For example, the interaction between the DMN and the salience network, which consists of anterior insula, dorsal anterior cingulate cortex, is associated with increased connectivity in amyloid-positive individuals with low neocortical tau, and decreased connectivity as a function of elevated Tau-PET signal (Schultz et al., 2017).

In addition to changes in the DMN, some studies have suggested that connectivity within the MTL is also disrupted with aging and AD. For example, Yassa et al. (Yassa et al., 2011a) showed an age-related decrease in connectivity between the entorhinal cortex and the dentate and CA3 regions of the hippocampus, the extent of which was correlated with memory deficits. Functional connectivity is thought to be an early marker of synaptic pathology that may be associated with isolation of the hippocampus from its cortical input.

Beyond the MTL network, the EC is interconnected with a broader neocortical network and is thought to provide the neural substrate for integrating spatial and object information (Ranganath and Ritchey, 2012). Evidence from the rodent indicates that the lateral entorhinal cortex is associated with cortical inputs including the orbitofrontal cortex and the amygdala while the medial entorhinal cortex is associated with cortical inputs such as the retrospenial cortex and postrhinal cortex, among others (Witter et al., 2017). It is thought that the functions of each of

these regions are, in part, due to their connections with these cortical inputs. However, how these regions and their computations are altered in Alzheimer's disease is not understood.

The RSC plays a key role in spatial memory and navigation, which means that this area represents a very important node in a broader spatial processing that includes the HF. The retrosplenial cortex (RSC) serves as a source of substantial, direct input to the EC, and projections from RSC account for nearly 20% of the total cortical input to the EC (Insausti et al., 1987). Neuroanatomical tracing data in the nonhuman primate show that the RSC has strong connections with the EC. Afferents to the EC originate in both Broca's area 29 and 30. Although these projections are restricted to the caudal one-half of the EC (E_I, E_C and E_{CL} subfields), whereas the rostral one-half of the EC receives little to no projections from the RSC. RSC afferents to the EC terminate mostly in layer I in a restricted topographical manner (Insausti and Amaral, 2008). Retrograde transport studies have shown that both PRC [area 35] (Kobayashi and Amaral, 2003) and PHC [areas TH and TF] project to RSC as well (Kobayashi and Amaral, 2003).

1.3.5 Memory systems and PMAT networks

Although episodic memory is supported by the circuitry of the medial temporal lobes (MTL), including the hippocampus, the MTL interacts extensively with a number of specific distributed cortical and subcortical structures (Dickerson and Eichenbaum, 2010). Spatial and nonspatial information seem to follow distinct parallel processing streams through the medial temporal lobes, with the hippocampus combining spatial and non-spatial information to form unified cohesive representations of an experience (Inhoff and Ranganath, 2017; Ranganath and Ritchey, 2012). In this model, spatial processing relies on a posteromedial (PM) system that includes the

entorhinal cortex, parahippocampal cortex, retrosplenial cortex, and posterior cingulate cortex, whereas object processing relies on an anterior-temporal (AT) system that includes the perirhinal cortex, the medial prefrontal cortex, and the anterior cingulate. Previous MRI studies have indicated early deterioration of anterior-temporal regions in aging that is linked to deficits in object memory (Berron et al., 2018; Reagh et al., 2018). Less attention has focused on the structural and functional integrity of the PM network. This is of importance to AD since the PM network is one of the earliest regions to show aggregation of beta-amyloid (Aβ) pathology (Klunk et al., 2004; Palmqvist et al., 2017). Furthermore, functional MRI studies have reported amyloid-β-related hyperactivation in hippocampus and posterior-medial regions that seems to reflect a failure in task-related deactivation (Elman et al., 2014; Huijbers et al., 2014; Leal et al., 2017; Mormino et al., 2012; Sperling et al., 2009; Vannini et al., 2012).

1.3.6 Mild cognitive Impairment and Alzheimer's Disease

One of the most common features of AD is decline in the ability to encode and retrieve our daily personal experiences, or episodic memory. A crucial component of episodic memory is pattern separation, the ability to independently represent and store similar experiences using unique neural codes (Marr, 1971; McClelland et al., 1995; Treves and Rolls, 1994; Yassa and Stark, 2011). Accumulating evidence suggests that the hippocampus possesses unique circuitry that is computationally capable of resolving mnemonic interference by using pattern separation (Leal and Yassa, 2018). This computation prevents overgeneralization of information and allows for efficient storage of episodic memories. Moreover, functional integrity of the hippocampus and decline in episodic memory can be attributed to loss of pattern separation (Leal and Yassa, 2015). Cognitive studies in aged humans have now reliably reported mnemonic discrimination

impairment (Stark et al., 2010, 2013; Yassa et al., 2011b) with more dramatic loss in aMCI (Bakker et al., 2012; Yassa et al., 2010).

Spatial memory is a special case of episodic memory that is known to be compromised very early in individuals with Alzheimer's disease (Hope et al., 1994; Lithfous et al., 2013), including in preclinical AD (Allison et al., 2016). In healthy brains of both humans and rodents, place cells in the hippocampus and grid cells in the medial entorhinal cortex (MEC) form a neural circuit that is critical for spatial memory (Doeller et al., 2010b; Ekstrom et al., 2003; Fyhn et al., 2004; Morris et al., 1982; O'Keefe and Dostrovsky, 1971; Scoville and Milner, 1957; Steffenach et al., 2005). The MEC, in particular, contains a high percentage of spatially modulated neurons such as grid, head direction, border, aperiodic spatial and object-vector cells (parameters necessary for spatial navigation) (Doeller et al., 2010b; Hafting et al., 2005; Jacobs et al., 2013; Killian et al., 2012; Miao et al., 2017; Sargolini et al., 2006; Solstad et al., 2008). Recent evidence has pointed to alterations in the neural coding properties in these networks in AD patients (Jun et al., 2020; Kunz et al., 2015).

CHAPTER 2: Establishing convergent validity of spatial pattern separation

Introduction

Remembering where you saw something is important for future behavior. Previous studies have demonstrated that mnemonic discrimination tasks are sensitive to hippocampal pattern separation, including the spatial pattern separation task. Word list recall is a standard memory task that is widely used in the clinical setting. In the current study, our goal was to establish convergent validity with a standardized memory task that is often used in a clinical setting. We hypothesized that the spatial pattern separation performance would be associated with a

standardized word list recall memory task. The current investigation builds on prior work by further specifying the nature of the memory phenotype associated with spatial pattern separation (e.g., learning vs. interference vs. retention).

Materials and Methods

Participants

A total sample of 84 older adults between 61 and 91 years of age (54 F, mean age = 73.3 years, SD = 6.10 years) were included in this study. Forty-five older adults were recruited from the Alzheimer's Disease Research Center (ADRC) Longitudinal Cohort at the University of California, Irvine and 39 were recruited from the surrounding Orange County community as part of the Biomarker Exploration in Aging, Cognition, and Neurodegeneration (BEACoN) study. Participants gave written informed consent in accordance with the Institutional Review Board of the University of California, Irvine, and were compensated for their participation.

Participants in the ADRC subsample (n = 45) were administered the Uniform Data Set (UDS-3) battery by a neuropsychologist in order to characterize the sample in accordance with the National Alzheimer's Coordinating Center (NACC) criteria (Weintraub et al., 2018). This is a standardized set of neuropsychological tests used by Alzheimer's Disease Centers across the United States. The battery includes the Montreal Cognitive Assessment (Nasreddine et al., 2005). Craft Story (Craft et al., 1996), Digit Span (Weschler, 1987), Trail making Test Parts A and B (Reitan and Wolfson, 1985), and the Benson Complex Figure Test (Possin et al., 2011). For statistical comparison between groups, participants were dichotomized into cognitively normal (CN) or cognitively impaired (CI), which include Mild Cognitively Impaired (MCI) and Cognitively Impaired, Non-Demented (CIND) participants. All participants (n = 84) were

administered the spatial pattern separation task, Rey Auditory Verbal Learning Test (RAVLT), Mini-Mental State Exam (MMSE). Seven participants from the ADRC subsample were excluded from analysis due to confusion with the task instructions.

Neuropsychological testing

The spatial pattern separation task was an optimized version of a paradigm previously developed by our group (Reagh et al., 2014, 2016, 2018). Participants first studied the location of objects during an incidental encoding task with an "Indoor or Outdoor" judgement. A surprise test phase was subsequently conducted during which participants viewed the same images again, half of which were presented in the same locations (targets) and half were presented in different locations (lures). Participants were asked to judge "Same" to correctly identify nondisplaced targets or "Different" to correctly identify displaced lures. The Spatial Lure Discrimination Index (LDI) was calculated as the proportion of lures correctly identified as "Different" minus the proportion of targets incorrectly identified as "Different" to correct for response bias. The Rey Auditory Verbal Learning Test (RAVLT) is a standard memory test that was developed to assess a variety of memory processes and assesses rate of learning, retention after short- and long-delay intervals, and recognition memory. We chose to focus on the RAVLT Delayed Recall component of the test (out of 15), as this has been shown to be sensitive to cognitive decline and episodic memory deficits with age (Andersson et al., 2006; Vakil and Blachstein, 1997). We have also previously reported correlations between spatial pattern separation performance and RAVLT word list delayed recall in older adults (Reagh et al., 2014), further motivating our use of this measure here to provide convergent validity for the spatial pattern separation task.

Results

Spatial pattern separation is associated with word list recall

A schematic of the spatial pattern separation task is shown in **Figure 3A**, and a more detailed description can be found in the Methods. Briefly, participants made discrimination/recognition judgments on items that were displaced from their original locations during study. The Spatial Lure Discrimination Index (LDI) was used as a summary measure of their performance. See Methods for details. Demographic information about the participants is displayed in **Table 1**.

Demographics		
	Full Sample	**CSF subsample**
Sample Size	77 (54 F)	38 (24 F)
Age (years)	73.3 (6.10)	74.5 (6.22)
Education (years)	16.5 (2.51)	16.2 (2.58)
Race		
White	59 (76.6%)	34 (89.5%)
Asian	15 (19.5%)	4 (10.5%)
Black or African American	1 (1.3%)	0 (0%)
More than One Race	2 (2.6%)	0 (0%)
Ethnicity		
Hispanic	4 (5.2%)	1 (2.6%)
Non-Hispanic	73 (94.8%)	37 (97.4%)
Diagnosis		
Normal (n)	67 (52 F)	28 (22 F)
Impaired (QCI, MCI) (n)	10 (2 F)	10 (2 F)
Baseline MMSE	28.2 (1.52)	28.3 (1.50)
RAVLT – learning slope	1.51 (0.543)	1.73 (0.616)
RAVLT – retroactive interference	0.829 (0.180)	0.798 (0.181)

RAVLT – percent forgetting	0.184 (0.219)	0.242 (0.257)
RAVLT – delayed recall	10.5 (3.59)	9.66 (4.05)
Aβ42/Aβ40	0.071 (0.025)	0.071 (0.205)
t-tau (pg/mL)	405 (266)	405 (266)
p-tau181 (pg/mL)	55.6 (46.0)	55.6 (46.0)

Table 1: Demographics and neuropsychological test scores. Unless otherwise stated, variables denote mean (± SD). Subjects in the CSF subsample were part of the full sample.

Consistent with our prior work, we observed a significant correlation between Spatial LDI and delayed recall performance (Pearson's $r = 0.301$, $p = 0.008$; **Figure 3B**). In considering covariates, we observed that sex and clinical status were highly correlated in this sample (Pearson $r = 0.423$, $p < 0.001$), as the cognitively impaired sample was predominantly male. Since our past work with pattern separation tasks had not observed sex differences in performance, we opted to only include age and clinical status as covariates in multiple regression. The overall model was statistically significant ($r = 0.531$, $F_{(3,73)} = 9.54$, $p < 0.001$), revealing a significant main effect of clinical status ($B = -4.059$, SE = 1.106, $t = -3.671$, $p < 0.001$). Spatial LDI ($B = 2.553$, $SE = 1.377$, $t = 1.854$, $p = 0.068$) and age ($B = -0.115$, $SE = 0.060$, $t = -1.910$, $p = 0.060$) were only marginally significant once clinical status was accounted for.

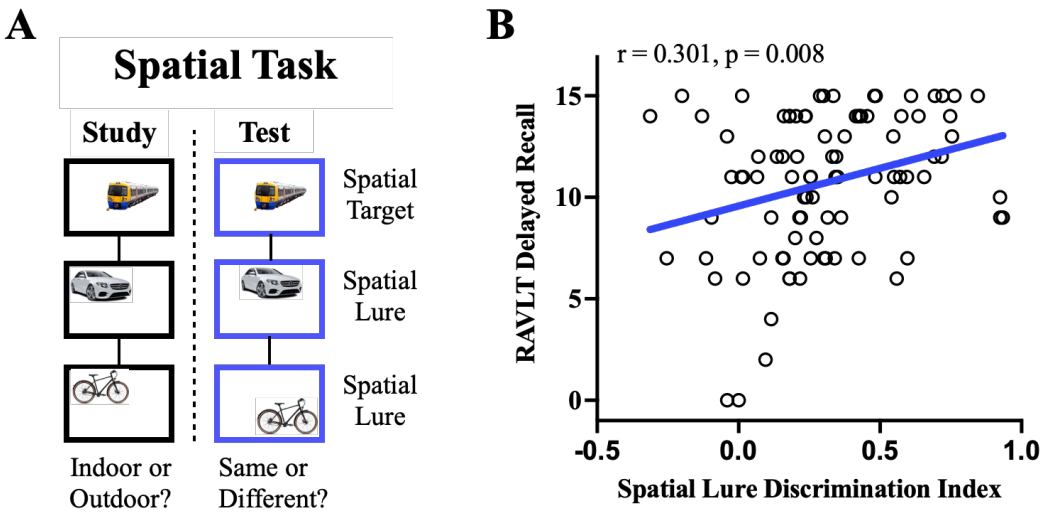

Figure 3. Spatial lure discrimination is associated with RAVLT delayed recall. (A) Schematic of the task. Participants first completed an encoding task with an incidental "Indoor or Outdoor" judgment, during which location objects were studied. Subsequently, a surprise test phase was conducted during which participants observed identical targets, and similar lure items with varying displacements. Subjects were asked to judge "Same or Different" with the former judgment accurately identifying targets and the latter accurately rejecting lures. (B) Spatial Lure Discrimination Index was related to performance on the RAVLT Delayed Recall (Pearson $r = 0.301$, $p = 0.008$).

To determine whether Spatial LDI was more specifically associated with measures that may be more sensitive to robustness again interference, retention across a delay, or learning across trials, we further assessed the relationship between Spatial LDI and other measures of memory and learning performance derived from the RAVLT. We calculated indices for (1) *retroactive interference* (List A Trial 6/List A Trial 5), a measure of whether new learning is inhibiting recall of previously learned information (Loewenstein et al., 2004; Yeung et al., 2019), (2) *percent forgetting* ([List A Trial 5 – List A Trial 7] / [List A Trial 5]), a measure of retention over the delay period (Estévez-González et al., 2003; Moradi et al., 2015, 2017), and (3) *learning slope* ([List A Trial 5 – List A Trial 1] / 4), a measure of learning over multiple trials.

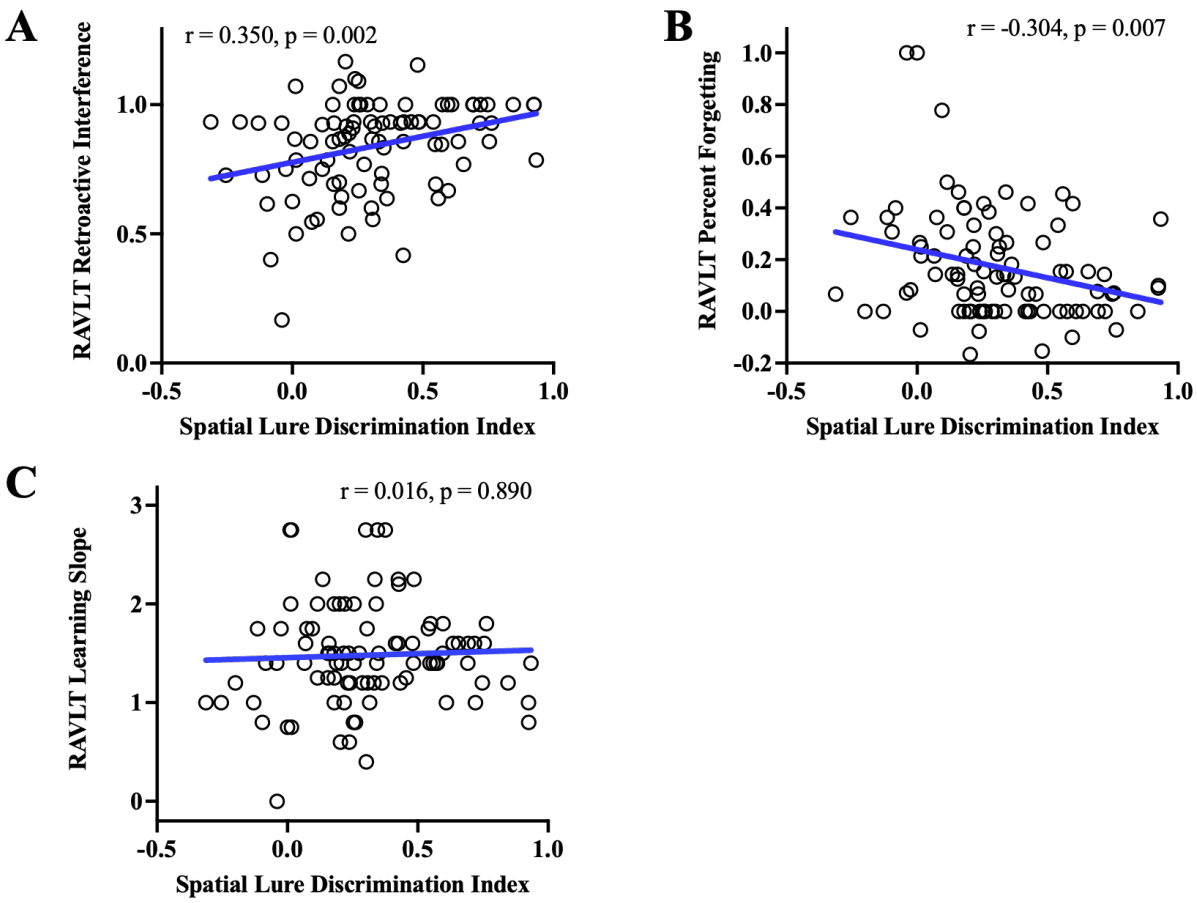

Figure 4. Spatial lure discrimination is associated with Retroactive Interference. (A-C) A higher Spatial LDI was related to higher Rey Auditory Verbal Learning Test (RAVLT) *retroactive interference* (Pearson $r = 0.350$, $p = 0.002$). A higher Spatial LDI was related to lower Rey Auditory Verbal Learning Test (RAVLT) *percent forgetting* (Pearson $r = -0.304$, $p = 0.007$). Spatial LDI was not associated with Rey Auditory Verbal Learning Test (RAVLT) *learning slope* (Pearson $r = 0.016$, $p = 0.890$).

We found that Spatial LDI was positively associated with *retroactive interference* scores (**Figure 4A**; Pearson $r = 0.350$, $p = 0.002$). We further assessed this relationship using multiple linear regression with age and clinical status as covariates. The overall model was statistically significant ($r = 0.425$, $F_{(3,73)} = 5.354$, $p = 0.002$), revealing a significant main effect of Spatial LDI ($B = 0.193$, $SE = 0.073$, $t = 2.654$, $p = 0.010$) and clinical status ($B = -0.126$, SE = 0.059, $t = -2.149$, $p = 0.035$). Age ($B = -0.001$, $SE = 0.003$, $t = -0.424$, $p = 0.673$) was not a significant

predictor. These results suggest that Spatial LDI and clinical status were significantly associated with neuropsychological measures *retroactive interference*.

We also found that higher Spatial LDI was related to lower *percent forgetting* (**Figure 4B**; Pearson r = -0.304, p = 0.007). We further assessed this relationship using multiple linear regression with age and clinical status as covariates. The overall model was statistically significant (r = 0.480, $F_{(3,73)}$ = 7.28, p < 0.001), revealing a significant main effect of clinical status (B = 0.206, SE = 0.069, t = 2.988, p = 0.004). Spatial LDI (B = -0.171, SE = 0.086, t = -1.985, p = 0.051) was only a marginally significant predictor and age (B = 0.006, SE = 0.004, t = 1.596, p = 0.115) was not a significant predictor. We found that Spatial LDI was not associated with learning slope (**Figure 4C**; Pearson r = 0.016, p = 0.890). Overall, this suggests that Spatial LDI is generally more associated with memory interference as opposed to learning or retention-related deficits per se.

Discussion

In a sample of nondemented older adults, we found that performance on a spatial pattern separation task was associated with RAVLT retroactive interference in word list recall. RAVLT is a standard neuropsychological test of episodic memory and retroactive interference is assumed to rely at least partially on the integrity of the hippocampus, providing a strong case for its use in assessing memory function (Kuhl et al., 2010; Wagner et al., 2016). We note the RAVLT is widely used for cognitive assessment in pre-dementia and dementia in a clinical setting, and is helpful for discriminating normally aging individuals from those with mild cognitive impairment (MCI) and AD (Balthazar et al., 2010).

Our previous work demonstrated that a subset of older adults who scored outside of the young norms on RAVLT delayed word list recall (but within age-matched norms) were significantly impaired on spatial pattern separation compared to older adults scoring within young adult norms as well as young adult groups (Reagh et al., 2014, 2016, 2018; Stark et al., 2010). This suggests that the task is sensitive to individual differences with aging. We note that in these studies spatial pattern separation performance was significantly correlated with word list recall scores in older adults, but not in young adults, although this could be driven by the reduced variability in recall scores in young adults.

Here, we extend and build on prior work by further specifying the nature of the memory phenotype associated with spatial pattern separation (e.g., learning vs. interference vs. retention). We calculated learning slope, retroactive interference, and percent forgetting scores. We showed that the Spatial LDI was significantly associated with retroactive interference, but not with percent forgetting or learning slope suggesting that performance on the spatial pattern separation task is more likely driven by interference rather than learning or retention deficits. This is consistent with prior studies demonstrating that aMCI patients are more susceptible to retroactive interference effects than cognitively normal older adults with a task similar to the RAVLT (Crocco et al., 2014).

Overall, our results suggest that spatial pattern separation is a sensitive marker of memory, and in particular, to the robustness of memory across interference. This is perhaps not surprising, since pattern separation is a computational mechanism that allows us to overcome interference from similar experiences (Yassa and Stark, 2011).

CHAPTER 3: Spatial pattern separation and PMAT framework

Introduction

Cortical pathways to the hippocampus appear to extend from two large-scale cortical systems: a posteromedial (PM) system that includes the parahippocampal cortex, retrosplenial cortex, and posterior cingulate cortex, and an anterior temporal (AT) system that includes the perirhinal cortex (Ritchey et al., 2015). The PMAT framework accounts for differences in the anatomical and functional connectivity of the medial temporal lobes. Using data-driven, graph theoretical analysis of resting-state functional connectivity data, networks strongly resembling PM and AT systems have been identified, in which connectivity was stronger within each network than between networks (Ritchey et al., 2014). Links between connectivity and function within the PM and AT networks have also been reported in task-activated fMRI studies, in which the PM system is associated with spatial processing and the AT system is associated with object processing, and temporal precision (Montchal et al., 2019; Reagh and Yassa, 2014). We hypothesized that PM functional connectivity would be associated with spatial pattern separation task performance.

Materials and Methods

Participants

Forty-five older adults between 61 and 91 years of age were recruited from the Alzheimer's Disease Research Center (ADRC) Longitudinal Cohort at the University of California, Irvine. Participants gave written informed consent in accordance with the Institutional Review Board of the University of California, Irvine, and were compensated for their participation. Participants were administered the Uniform Data Set (UDS-3) battery by a neuropsychologist in order to

characterize the sample in accordance with the National Alzheimer's Coordinating Center (NACC) criteria (Weintraub et al., 2018). This is a standardized set of neuropsychological tests used by Alzheimer's Disease Centers across the United States. The battery includes the Montreal Cognitive Assessment (Nasreddine et al., 2005). Craft Story (Craft et al., 1996), Digit Span (Weschler, 1987), Trail making Test Parts A and B (Reitan and Wolfson, 1985), and the Benson Complex Figure Test (Possin et al., 2011). For statistical comparison between groups, participants were dichotomized into cognitively normal (CN) or cognitively impaired (CI), which include Mild Cognitively Impaired (MCI) and Cognitively Impaired, Non-Demented (CIND) participants.

All participants (n = 45) were administered the spatial pattern separation task, Rey Auditory Verbal Learning Test (RAVLT), Mini-Mental State Exam (MMSE). Seven participants from the ADRC subsample were excluded from analysis due to confusion with the task instructions. Participants in the ADRC subsample additionally underwent resting state fMRI imaging. Of the 38 participants in the ADRC subsample, two participants were excluded in the imaging analyses due to poor signal in the medial temporal lobes.

MRI data acquisition

Neuroimaging data were acquired on a 3.0 Tesla Philips Achieva scanner, using a 32-channel sensitivity encoding (SENSE) coil at the Neuroscience Imaging Center at the University of California, Irvine. A high-resolution 3D magnetization-prepared rapid gradient echo (MP-RAGE) structural scan (0.65 mm isotropic voxels) was acquired at the beginning of each session and used for co-registration. For each subject, resting state EPI scans consisted of a T2*-weighted echo planar imaging (EPI) sequence using blood-oxygenation-level-dependent (BOLD) contrast: repetition time (TR)=3500 ms, echo time (TE)=26 ms, flip angle=70 degrees, 55 slices,

100 dynamics per run, 1.8 x 1.8 mm in plane resolution, 1.8 mm slice thickness with a 0.2 mm gap, field of view (FOV)=180x109.8x180. Slices were acquired as a partial axial volume and without offset or angulation. Four initial "dummy scans" were acquired to ensure T1 signal stabilization.

MRI data preprocessing

All neuroimaging data were preprocessed and analyzed using Analysis of Functional NeuroImages (AFNI) (Cox, 1996). on GNU/Linux and Mac OSX platforms. Analyses largely took place in accordance with the standardized afni_proc.py pipeline. Specifically, data were corrected for motion (3dvolreg) and slice timing shifts (3dTshift), masked to exclude voxels outside the brain (3dautomask), and were smoothed (3dmerge) to a 2.0mm using a Gaussian FWHM kernel. Each run was also despiked to further reduce the influence of motion on the data (3dDespike). Functional scans were aligned to each subject's skull-stripped MP-RAGE (align-epi_anat.py). We defined ROIs based on our prior work (Reagh and Yassa, 2014; Yushkevich et al., 2015). We used Advanced Normalization Tools (ANTS) (Avants et al., 2008) to warp each individual participant's MP-RAGE structural scan into our custom in-house high-resolution template space using nonlinear, diffeomorphic transformation. Parameters from these warps were used to also warp functional scans into template space for group analyses. Masks were resampled to match the resolution of the fMRI data (1.8x1.8.x2.0mm) and were further masked to exclude partially sampled voxels within and across runs (3dcalc). Once we obtained models of ongoing BOLD activity per subject (3dDeconvolve), we extracted the average time course across ROIs (3dmaskave). A Fisher's r-to-z transformation was applied to each correlation map, to obtain an approximately normal distribution of the functional connectivity values and accordingly apply parametric statistics (3dcalc). PHC, and RSC ROIs were generated from masks used previously

by our group (Reagh and Yassa, 2014). Other cortical ROIs were merged with our mask based on the Freesurfer cortical atlas (Dale et al., 1999; Fischl et al., 1999). To assess functional connectivity, we calculated the Pearson correlation coefficient between the mean signal intensity time courses of each ROI pair.

Statistical analysis

All statistical analyses on voxel-averaged data and data visualizations were conducted in Jamovi (Version 1.6.23.0), R (version 3.6.3) and GraphPad Prism (Version 8.4.3). Preprocessing and first-level analyses of neuroimaging data were conducted in AFNI (Version 16.0) using the functions described throughout the Methods section.

Results

Spatial pattern separation is associated with PM network functional connectivity

A subset (n=36) of our participants underwent resting state functional MRI scans, allowing us to assess the relationship between spatial pattern separation and functional connectivity in the PMAT system. Since our hypotheses were specific to PM regions, we conducted region of interest (ROI) analyses in PM and AT cortex and assessed whether resting state fMRI functional connectivity among regions constituting these networks is associated with spatial pattern separation task performance. Correlation coefficients were calculated between the mean signal intensity time courses of each ROI pairs were calculated. ROIs are shown in **Figure 5A**. Regression coefficients were then averaged across all ROI pairs to determine the PM functional connectivity and AT functional connectivity. See Methods for details on how fMRI data were processed and analyzed.

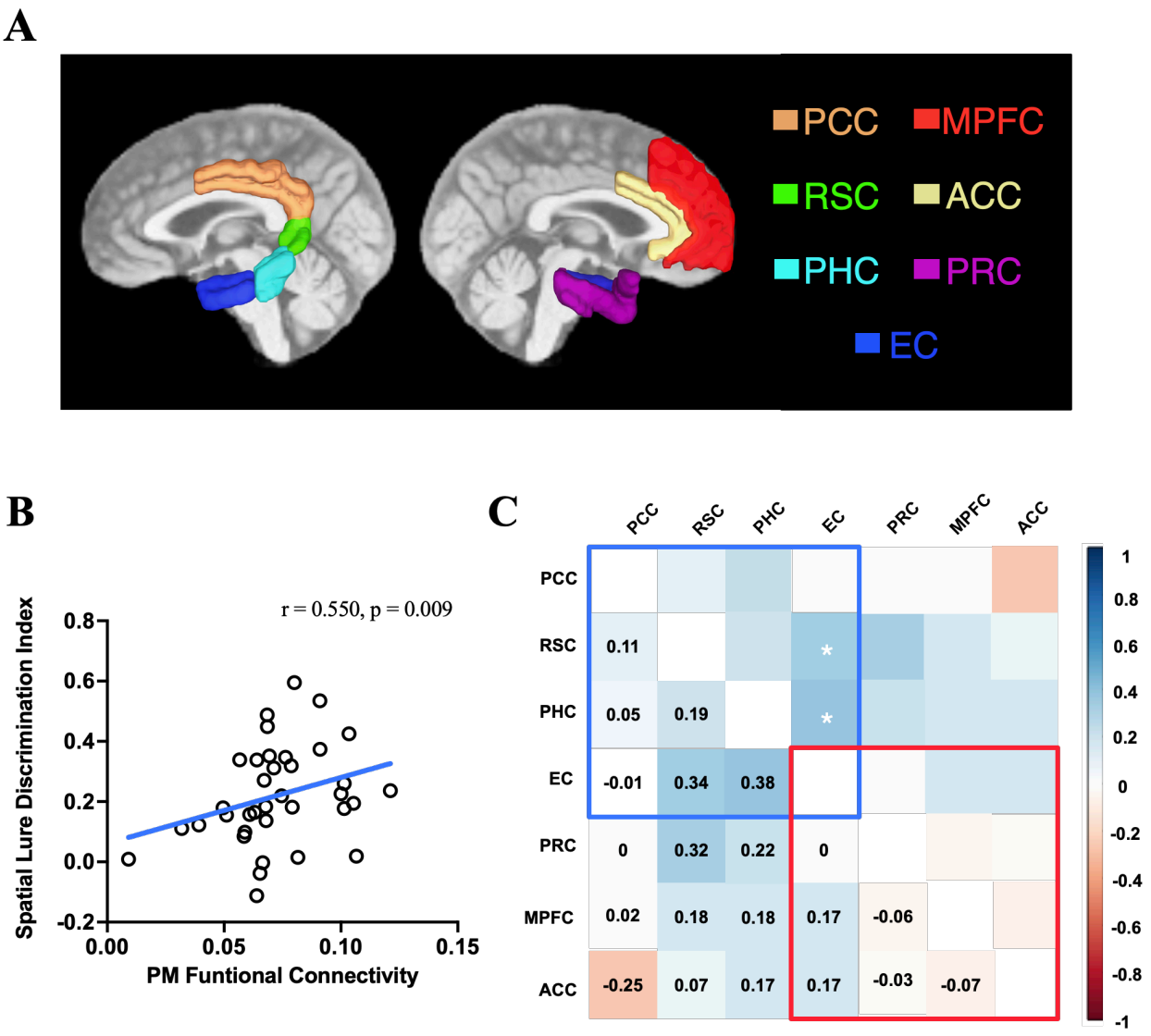

Figure 5. Functional connectivity of the posteromedial system associated with Spatial Lure Discrimination Index (A) Anatomical regions of interest (ROIs) used to mask functional data. ROIs were generated from masks used previously by our group (PCC = posterior cingulate cortex, RSC = retrosplenial cortex, PHC = parahippocampal cortex, EC = entorhinal cortex, PRC = perirhinal cortex, mPFC = medial prefrontal cortex, ACC = anterior cingulate cortex). (B) Higher Spatial LDI was related to higher functional connectivity across posteromedial (PM) regions ($r = 0.550$, $p = 0.008$). (D) Functional connectivity of each pairwise correlation, with PM connectivity shown in the blue square and AT connectivity shown in the red square. Asterisks indicate that the correlation is significant ($p < 0.05$).

We conducted two multiple regressions. First, we assessed the relationship between PM functional connectivity and Spatial LDI, with age and clinical status as covariates. The overall

model was statistically significant ($r = 0.550$, $F_{(3,32)} = 4.62$, $p = 0.009$; **Figure 5B**), revealing PM functional connectivity ($B = 2.601$, $SE = 1.083$, $t = 2.40$, $p = 0.022$), and age ($B = -0.008$, $SE = 0.004$, $t = -2.15$, $p = 0.039$) were significant predictors of Spatial LDI. Clinical status was only a marginal predictor of Spatial LDI ($B = -0.110$, SE = 0.054, $t = -2.03$, $p = 0.051$). Second, we assessed the specificity of this relationship by conducting a multiple regression to test whether AT functional connectivity predicted Spatial LDI, covarying for age and clinical status. The overall model was statistically significant ($r = 0.487$, $F_{(3,32)} = 3.31$, $p = 0.032$). However, neither AT functional connectivity ($B = 2.982$, $SE = 1.878$, $t = 1.59$, $p = 0.122$), nor age ($B = -0.008$, $SE = 0.004$, $t = -1.92$, $p = 0.063$) or clinical status ($B = -0.114$, SE = 0.058, $t = -1.99$, $p = 0.056$) were significant predictors of Spatial LDI. Overall, this suggests that spatial pattern separation is associated with PM, but not AT functional connectivity. **Figure 5C** shows the matrix of individual ROI-pair correlations. PM connectivity is shown in the blue square and AT connectivity is shown in the red square.

Discussion

We have previously shown that object and spatial pattern separation engage parallel networks in the rhinal cortex, which are extensions of the PM and AT networks. Specifically, object pattern separation engaged the perirhinal and lateral entorhinal cortices (components of the AT network), while spatial pattern separation engaged the parahippocampal and medial entorhinal cortices (components of the PM network) (Reagh and Yassa, 2014). Recent fMRI studies have also demonstrated age-related deficits in object-related processing related to lateral entorhinal cortex hypoactivity (Berron et al., 2018; Reagh et al., 2018) and to dysfunction of the AT system (Maass et al., 2018). However, an important and open question is to understand how dysfunction of the PM network is linked to spatial pattern separation. Our results here address this question

by showing that spatial pattern separation is associated with functional connectivity of the larger PM network. Interestingly, we do not observe the same associations with AT network connectivity. Overall, these results suggest that spatial pattern separation is a sensitive measure of cognitive change in older adults that have higher levels of pathological aggregates (Aβ and t-tau) and is associated with functional connectivity in the PM network, which is implicated in spatial memory processing.

Recent evidence has suggested that AD pathologies differentially target these networks, with Aβ preferentially targeting the PM network and tau preferentially targeting the AT network (Maass et al., 2019). Several studies have also suggested that in the presence of neocortical Aβ plaques, tau pathology in the temporal lobe further increases but also 'spreads' to posteromedial regions (Leal et al., 2018; Lockhart et al., 2017; Vemuri et al., 2017) where pathologies converge. Thus, an emerging view from recent studies suggest that amyloid potentiates the spread of tau into neocortical regions (Schwarz et al., 2016). These regional relationships could not be assessed directly here, since CSF measures do not offer insights into network-specific distributions of pathology, however, future work with longitudinal PET imaging can be used to further shed light on these relationships.

CHAPTER 4: Spatial pattern separation and Alzheimer's disease pathology

Introduction

While previous studies have reported spatial pattern separation deficits in older adults, these studies have been limited in examining the relationship between spatial pattern separation and Alzheimer's disease-related pathology. Previous studies have shown that regions involved in

spatial memory are early sites of Aβ pathology and that Aβ deposition is higher in PM regions than in AT regions (Koychev et al., 2020; Maass et al., 2019; Palmqvist et al., 2017). We hypothesized that amyloid pathology underlies spatial pattern separation performance deficits and alters in the functional connectivity of the PM network.

Materials and Methods

Participants

A total of 45 older adults between 61 and 91 years of age were included in this study. Forty-five older adults were recruited from the Alzheimer's Disease Research Center (ADRC) Longitudinal Cohort at the University of California, Irvine. Participants gave written informed consent in accordance with the Institutional Review Board of the University of California, Irvine, and were compensated for their participation. Demographic information about the participants is displayed in **Table 1**.

Participants were administered the Uniform Data Set (UDS-3) battery by a neuropsychologist in order to characterize the sample in accordance with the National Alzheimer's Coordinating Center (NACC) criteria (Weintraub et al., 2018). This is a standardized set of neuropsychological tests used by Alzheimer's Disease Centers across the United States. The battery includes the Montreal Cognitive Assessment (Nasreddine et al., 2005). Craft Story (Craft et al., 1996), Digit Span (Weschler, 1987), Trail making Test Parts A and B (Reitan and Wolfson, 1985), and the Benson Complex Figure Test (Possin et al., 2011). For statistical comparison between groups, participants were dichotomized into cognitively normal (CN) or cognitively impaired (CI), which include Mild Cognitively Impaired (MCI) and Cognitively Impaired, Non-Demented (CIND) participants.

All participants were administered the spatial pattern separation task, Rey Auditory Verbal Learning Test (RAVLT), Mini-Mental State Exam (MMSE). Seven participants from the ADRC subsample were excluded from analysis due to confusion with the task instructions. Cerebrospinal fluid (CSF) was obtained via lumbar puncture (n = 38).

Results

Spatial pattern separation is associated with CSF pathology

A subset (n=38) of our participants underwent CSF lumbar punctures, allowing us to assess the relationship between spatial pattern separation and AD pathological features. First, we confirmed that the previously identified behavioral relationship between task performance and RAVLT delayed recall was present in this subsample (Pearson $r = 0.509$, $p = 0.001$; **Figure 6A**). We considered three key CSF pathology measures, Aβ42/40 ratio, total tau (t-tau), and phospho-tau-181 (p-tau). Within our sample, Aβ42/40 ratio was correlated with t-tau (Pearson $r = -0.475$, $p = 0.003$), and p-tau (Pearson $r = -0.560$, $p < 0.001$). T-tau was also highly correlated with p-tau (Pearson $r = 0.961$, $p < 0.001$).

Adjusting for age, and clinical status, Aβ42/40 ratio was not directly correlated with Spatial LDI (partial $r = 0.108$, $p = 0.531$), but we observed a significant correlation between Aβ42/40 ratio and delayed recall scores (partial $r = 0.405$, $p = 0.014$; **Figure 6B**). We then examined the effect of Aβ42/40 as a potential moderator of the relationship between Spatial LDI and delayed recall using multiple linear regression with age and clinical status as covariates. The overall regression was statistically significant ($r = 0.769$, $F_{(5,32)} = 9.280$, $p < 0.001$). This model revealed significant main effects of Spatial LDI ($B = 28.715$, $SE = 9.251$, $t = 3.104$, $p = 0.004$), Aβ42/40 ($B = 12.082$,

SE = 3.547, *t*= 4.407, *p* = 0.002), and age (*B* = -0.225, *SE* = 0.084, *t* = -2.684, *p* = 0.011). The interaction between Spatial LDI and Aβ42/40 ratio was also significant (*B* = -27.842, *SE* = 11.803, *t*= -2.359, *p* = 0.025). Clinical status was not a significant predictor of delayed recall (*B* = -2.023, *SE* = 1.199, *t*= -1.687, *p* = 0.101). A simple slopes analysis for the relationship between Spatial LDI and delayed recall at upper, middle, and lower tertiles of Aβ42/40 shows the conditional effect by which Aβ42/40 moderates the relationship between Spatial LDI and RAVLT delayed recall (**Figure 6C**). Slopes and 95% confidence intervals for the relationship between Spatial LDI and delayed recall at upper, middle, and lower tertile of Aβ42/40 ratio levels show that the slope of Spatial LDI is significant only in the lower tertile (*B* = 25.60, *SE* = 5.85, *t* = 4.38, *p* < 0.001), but not the upper (*B* = 5.36, *SE* = 4.76, *t* = 1.13, *p* = 0.27), or middle tertiles (*B* = 3.99, *SE* = 5.20, *t* = 0.77, *p* = 0.45; **Figure 6D**).

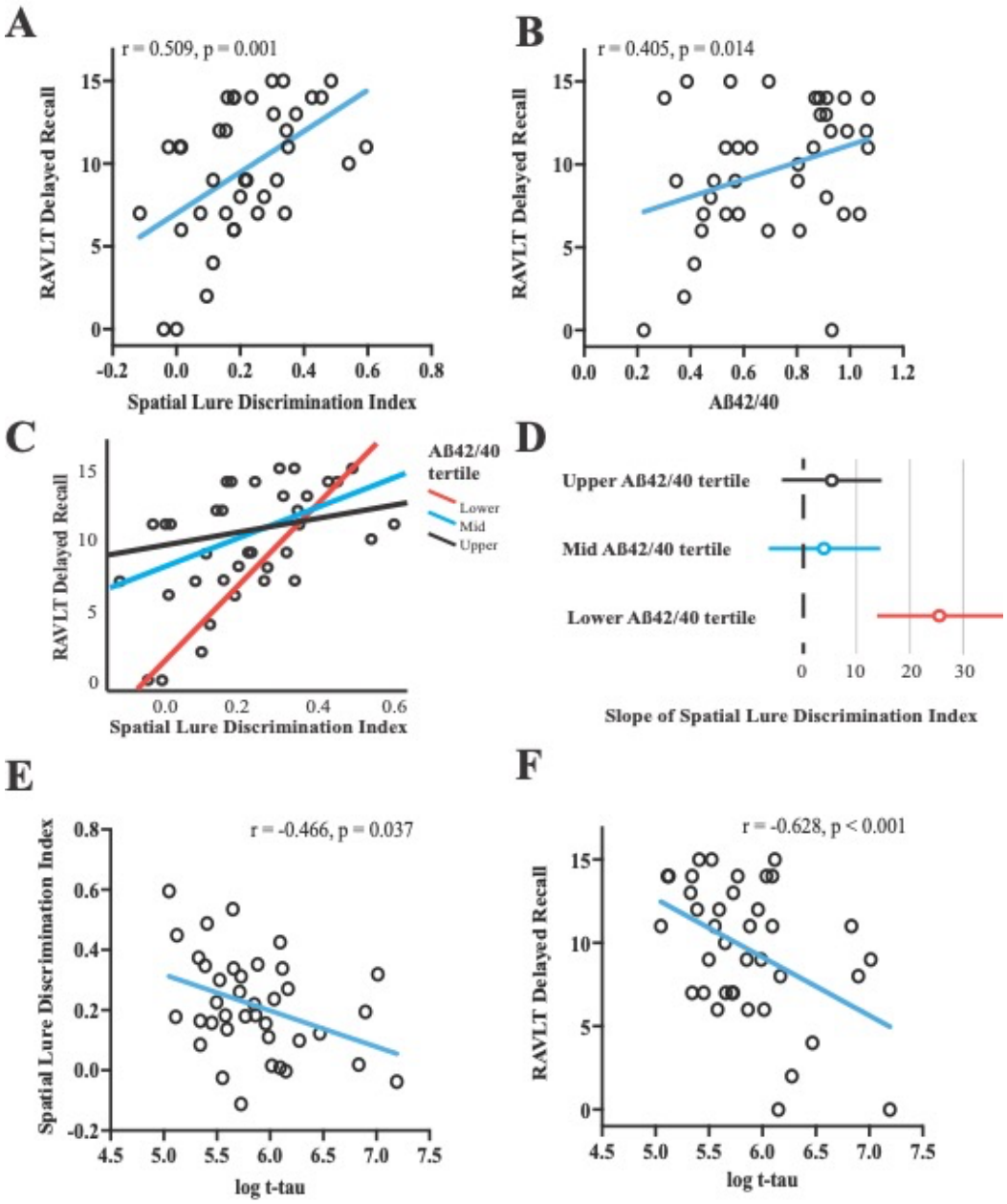

Figure 6. Relationship between CSF biomarkers, spatial lure discrimination index (LDI), and RAVLT delayed recall. (A) Higher Spatial Lure Discrimination Index (LDI) performance was related to better performance on the Rey Auditory Verbal Learning Test (RAVLT) delayed recall in the CSF subsample (Pearson $r = 0.509$, $p = 0.001$). (B) Lower Aβ42/40 is associated with worse performance on RAVLT Delayed Recall (partial $r = 0.405$, $p = 0.014$). (C, D) Slopes and 95% confidence intervals for relationship between Spatial LDI and RAVLT delayed recall at upper, middle, and lower tertiles of Aβ42/40 ratio levels. (E, F) Higher log-transformed levels of total tau (log-tau) were significantly related to worse performance on the Spatial LDI ($r = -0.466$, $p = 0.037$), and worse performance on the RAVLT Delayed Recall ($r = -0.628$, $p < 0.001$).

Next, we turned our attention to tau pathology measures. Since t-tau and p-tau levels were not normally distributed, we log-transformed them. First, we examined the relationship between log t-tau and Spatial LDI using multiple linear regression with age and clinical status as covariates. The overall model was significant (**Figure 6E**; $r = 0.466$, $F_{(3,34)} = 3.15$, $p = 0.037$), revealing a significant main effect of log t-tau ($B = -0.108$, $SE = 0.053$, $t = -2.045$, $p = 0.049$). Age ($B = -0.007$, $SE = 0.004$, $t = -1.619$, $p = 0.115$) and clinical status ($B = -0.037$, $SE = 0.062$, $t = -0.596$, $p = 0.555$) were not significant predictors. Then, we examined the relationship between log t-tau and RAVLT delayed recall using multiple linear regression with age and clinical status as covariates. The overall model was significant (**Figure 6F**; $r = 0.628$, $F_{(3,34)} = 7.38$, $p < 0.001$), revealing a significant main effect of log t-tau ($B = -0.005$, $SE = 0.002$, $t = -2.11$, $p = 0.042$), age ($B = -0.200$, $SE = 0.089$, $t = -2.24$, $p = 0.032$), and clinical status ($B = -2.933$, $SE = 1.373$, $t = -2.14$, $p = 0.040$).

We then repeated the same analyses for p-tau. We first examined the relationship between log p-tau and Spatial LDI using multiple linear regression with age and clinical status as covariates. The overall regression showed that log p-tau was associated with Spatial LDI ($r = 0.386$, $F_{(3,34)} = 1.98$, $p = 0.135$). Log p-tau ($B = -0.053$, $SE = 0.051$, $t = -1.045$, $p = 0.304$), age ($B = -0.006$, $SE = 0.004$, $t = -1.475$, $p = 0.150$), and clinical status ($B = -0.056$, $SE = 0.067$, $t = -0.842$, $p = 0.406$) were not significant predictors. Then, we examined the relationship between log p-tau and RAVLT delayed recall using multiple linear regression with age and clinical status as covariates. The overall regression showed that log p-tau was associated with delayed recall ($r = 0.628$, $F_{(3,34)} = 7.83$, $p < 0.001$), revealing a significant main effect of log p-tau ($B = -0.005$, $SE = 0.002$, $t = -2.11$, $p = 0.042$), age ($B = -0.200$, $SE = 0.089$, $t = -2.24$, $p = 0.032$), and clinical status ($B = -2.933$, $SE = 1.373$, $t = -2.14$, $p = 0.040$).

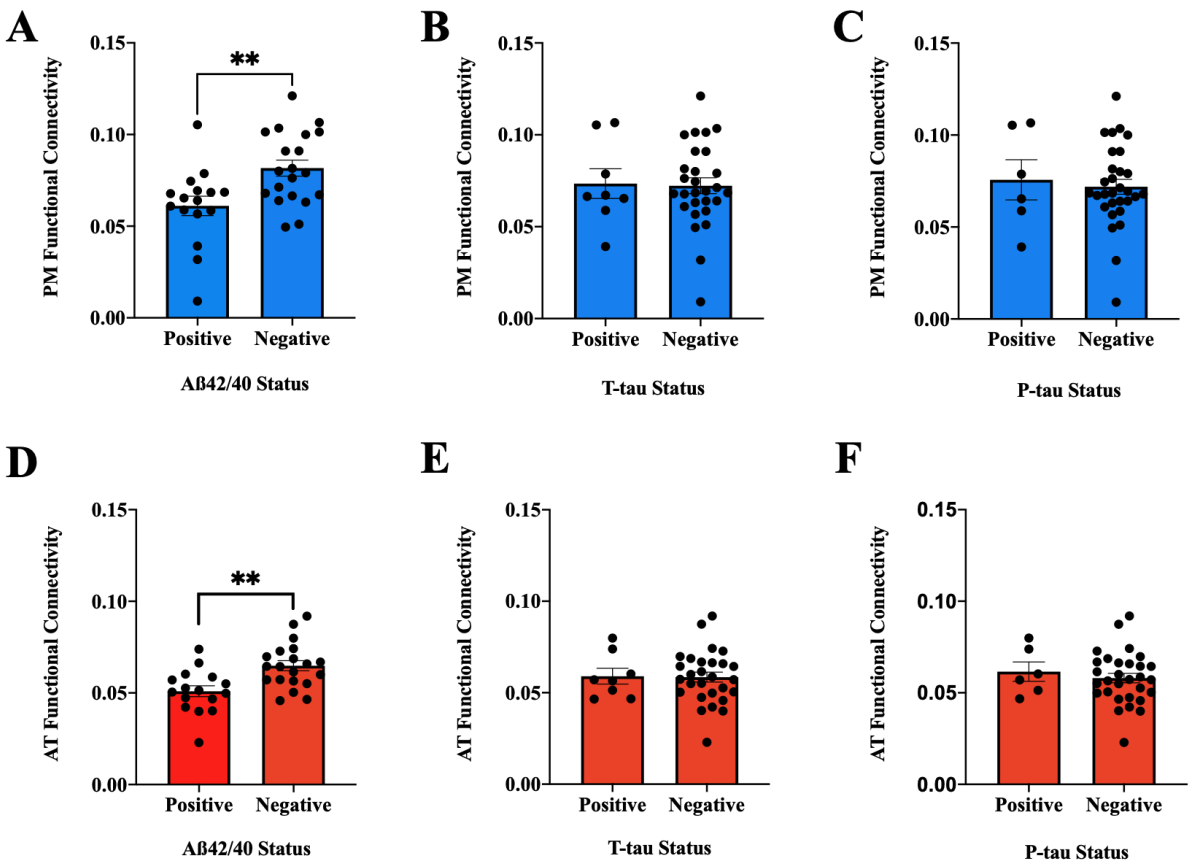

Figure 7. CSF biomarker group differences in functional connectivity. (A,D) A two-tailed two sample t-test showed that the Aβ positive group had lower PM functional connectivity that the Aβ negative group ($t_{(34)}$ = 3.014, p = 0.005) and the Aβ positive group had lower AT functional connectivity than the Aβ negative group ($t_{(34)}$ = 3.418, p = 0.002). (B, C, E, F) No differences in PM or AT functional connectivity between positive and negative groups of groups of t-tau or p-tau.

We then examined the relationship between CSF pathology markers and PMAT functional connectivity. We dichotomized the sample based on published cutoffs for Aβ42/40, t-tau and p-tau and ran two-tailed two-sample t-tests to determine whether there are group differences in PMAT functional connectivity. We found that the Aβ positive group had lower PM functional connectivity ($t_{(34)}$ = 3.014, p = 0.005; **Figure 7A**) and lower AT functional connectivity ($t_{(34)}$ = 3.418, p = 0.002; Figure 6D) than the Aβ negative group. No significant t-tau or p-tau group differences in PM or AT functional connectivity were noted (**Figure 7B, C, E, F**).

Discussion

Neuropathologically, the presence of protein aggregates comprising of beta amyloid (i.e. neuritic plaques) and hyperphosphorylated tau (i.e. neurofibrillary tangles) are hallmark features of AD (Jack et al., 2018; McKhann et al., 2011). In AD, abnormal accumulation of amyloid and tau proteins in the brain is thought to begin 10–20 years before clinical symptom onset (Bateman et al., 2012; Hof et al., 1996; Perl, 2010). Currently, the predominant modalities for assessments of these pathologies are cerebrospinal fluid (CSF) and positron emission tomography (PET). CSF Aβ42 becomes abnormal in the earliest stages of AD before amyloid PET detection and before neurodegeneration starts (Palmqvist et al., 2016). Additionally, the concordance between CSF Aβ42 and amyloid PET imaging is high, but not perfect (Hansson et al., 2018; Schindler et al., 2018; Toledo et al., 2015). The ratio of Aβ42/40 has been shown to have better agreement with amyloid PET imaging compared to levels of Aβ42 alone (Alcolea et al., 2019; Janelidze et al., 2016, 2017; Lewczuk et al., 2017; Schindler et al., 2018). Previous studies have shown that CSF Aβ42/40 is a sensitive measure of Aβ plaques, CSF t-tau is a sensitive measure of neurodegeneration, and CSF p-tau is a biomarker associated with both the phosphorylation state of tau and neurofibrillary tangle formation (Blennow et al., 2010; Jack et al., 2018; Strozyk et al., 2003). It is important to also note that while t-tau and p-tau levels in CSF are thought to vary proportionately with brain pathology levels, Aβ measures in CSF are thought to vary inversely with brain pathology (i.e., the higher the CSF Aβ, the lower the brain Aβ; (Tapiola et al., 2009).

Our findings support the notion that while CSF measures have often been dichotomized into "positive" and "negative" based on reliable cutoffs (Jack et al., 2018), pathological burden can be conceptualized on a continuum with a progressively increasing risk of cognitive decline. Here

we show that RAVLT delayed recall is associated with Aβ42/40, t-tau, and p-tau. However, Spatial LDI is only directly associated with t-tau, but not Aβ42/40 or p-tau. Importantly, we showed that the relationship between Spatial LDI and RAVLT delayed recall is conditional upon the level of β-amyloid burden. This suggests Spatial LDI may be a more specific marker to the concurrent pathologies of AD, as its sensitivity to tau pathology is increased in the presence of lower levels of CSF Aβ (i.e. higher levels of brain Aβ).

The relationships among CSF pathology, functional connectivity in specific neural systems, and cognition may hold the key to better understanding of how early AD evolves in the aging brain. Considerable evidence suggests that pathological processes involving amyloid and tau affect brain network function, which in turn may affect cognitive performance (Huijbers et al., 2019; Marks et al., 2017; Mormino et al., 2012; Sperling et al., 2009). Converging evidence has demonstrated that two distinct cortical pathways converge in the hippocampus: the anterior-temporal (AT) network and the posteromedial (PM) network (Ranganath and Ritchey, 2012). While the AT network has been associated with object memory, the PM network has been associated with spatial and contextual memory (Ritchey et al., 2015). The involvement of the PM system in spatial processing and spatial memory has been reliably shown in past studies. For example, the PM network's retrosplenial cortex has been associated with spatial updating and orienting (Burles et al., 2017), as well as spatial navigation and path integration (Sherrill et al., 2013).

This study has a few limitations to consider. We cannot exclude the possibility that our results reflect sources of amyloid or tau hypothesized to be non-AD related, such as primary age-related tauopathy (Crary et al., 2014; Duyckaerts et al., 2015). As CSF measures of AD pathology are

not regionally specific, we cannot determine with certainty whether our findings are the result of local or regional effects of AD pathology.

CHAPTER 5: Spatial pattern separation and cognitive decline

Introduction

Given the clinical relevance of spatial memory deficits in early AD as well as the vulnerability of the PM network to amyloid pathology, we asked the question: Could a mechanistically validated spatial memory task be used as an early diagnostic or predictor of cognitive decline? To address this question, we tested a sample of nondemented older adults that includes cognitively normal and cognitively impaired individuals. We used a memory task tailored to probe spatial pattern separation, a high-precision form of object-location association and hypothesized that performance on the task would predict longitudinal cognitive decline.

Materials and Methods

Participants

A total sample of 45 older adults between 61 and 91 years of age were included in this study. Forty-five older adults were recruited from the Alzheimer's Disease Research Center (ADRC) Longitudinal Cohort at the University of California, Irvine. Participants gave written informed consent in accordance with the Institutional Review Board of the University of California, Irvine, and were compensated for their participation.

Participants were administered the Uniform Data Set (UDS-3) battery by a neuropsychologist in order to characterize the sample in accordance with the National Alzheimer's Coordinating Center (NACC) criteria (Weintraub et al., 2018). This is a standardized set of neuropsychological

tests used by Alzheimer's Disease Centers across the United States. The battery includes the Montreal Cognitive Assessment (Nasreddine et al., 2005). Craft Story (Craft et al., 1996), Digit Span (Weschler, 1987), Trail making Test Parts A and B (Reitan and Wolfson, 1985), and the Benson Complex Figure Test (Possin et al., 2011). For statistical comparison between groups, participants were dichotomized into cognitively normal (CN) or cognitively impaired (CI), which include Mild Cognitively Impaired (MCI) and Cognitively Impaired, Non-Demented (CIND) participants.

All participants were administered the spatial pattern separation task, Rey Auditory Verbal Learning Test (RAVLT), Mini-Mental State Exam (MMSE). Seven participants from the ADRC subsample were excluded from analysis due to confusion with the task instructions. Longitudinal MMSE scores were obtained as part of a larger battery of tests used at an annual evaluation (n=37).

Results

Spatial pattern separation predicts annualized decline in MMSE scores

We assessed the predictive validity of spatial pattern separation by testing whether task performance predicted longitudinal cognitive decline. Demographic information about the participants is displayed in **Table 1**. Using the Mini-Mental State Exam (MMSE) as the key cognitive outcome of interest, we plotted the trend in individual subject scores over time relative to baseline MMSE score (**Figure 8A**). We calculated MMSE annualized percent change (MMSE APC) as the difference between the last MMSE score and the baseline MMSE score divided by time in between (in years). We found that baseline Spatial LDI was correlated with MMSE APC (Pearson $r = 0.545$, $p = 0.0005$; **Figure 8B**), but baseline RAVLT delayed recall scores (Pearson $r = 0.240$, $p = 0.152$; **Figure 8C**), and baseline MMSE scores (Pearson $r = -0.189$, $p = 0.262$;

Figure 7D) were not correlated with MMSE APC. We then assessed the relationship between Spatial LDI and MMSE APC using multiple regression with age, and clinical status as covariates. The overall model was significant ($r = 0.580$; $F_{(3,33)} = 5.48$, $p = 0.003$), demonstrating that baseline Spatial LDI remained significantly associated with MMSE APC ($B = 5.594$, $SE = 1.595$, $t = 3.508$, $p = 0.001$). Age ($B = 0.024$, $SE = 0.041$, $t = 0.583$, $p = 0.564$), and clinical status ($B = 0.752$, $SE = 0.588$, $t = -1.279$, $p = 0.210$) were not significant predictors.

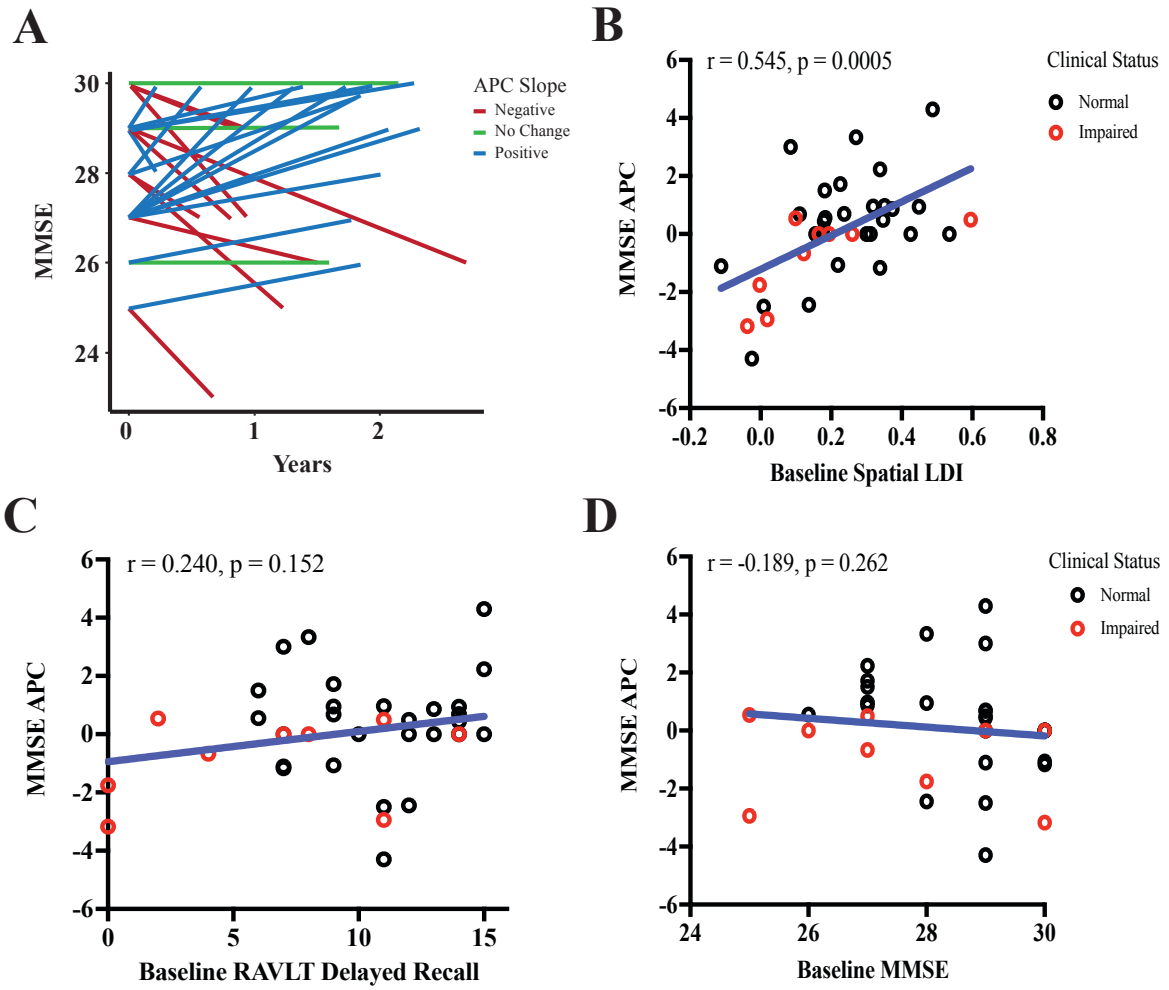

Figure 8. Spatial discrimination predicts annualized percent change of MMSE scores (MMSE APC). (A) MMSE distribution for each participant over time, relative to baseline MMSE score, where blue indicates positive changes, green indicates no change, and red represents negative changes. (B) Baseline Spatial LDI was significantly associated with MMSE APC (Pearson $r = 0.545$; $p = 0.0005$). (C) Baseline RAVLT Delayed Recall scores were not associated with MMSE APC (Pearson $r = 0.240$, $p = 0.152$). (D) Baseline MMSE scores were not associated with MMSE APC (Pearson $r = -0.189$, $p = 0.262$).

Discussion

Our results indicate that spatial pattern separation performance may be an informative measure with respect to the trajectory of cognitive decline. Here we demonstrate a relationship between spatial pattern separation performance at baseline and cognitive decline as assessed by decreases in MMSE scores over a 1–2-year period. These relationships were not present with baseline RAVLT delayed recall scores, which is a standard neuropsychological tool for evaluating memory function and decline. This speaks to the predictive validity of the task and the promise it holds for potential use in clinical trials. Furthermore, our participant sample consisted of mostly white, highly educated individuals, thus limiting the generalizability of results. Future work should attempt to reproduce these findings in community-based samples drawn from ethnically diverse populations.

CHAPTER 6: Synthesis and Future Directions

General Summary

The goal of this dissertation was to investigate spatial memory networks in aging and Alzheimer's disease. To investigate the neurobiological mechanisms involved, a series of experiments establish relationships between spatial pattern separation and the functional connectivity of spatial memory networks, AD pathology, and clinical measures of cognitive impairment and decline. Overall, we find that applying a pattern separation framework to the changes involved in spatial memory offers a potential mechanistic account for how spatial memory is affected in the context of Alzheimer's disease. For the next sections, I will summarize the results from the experiments presented and discuss their impact and relevance more broadly.

Vulnerability of the PM network

These findings suggest that older adults may have distinct changes occurring in the PMAT networks that are dependent on the content of the memory being recalled. Previous work reports that the spatial pattern separation task to probe spatial memory with a high level of fidelity in older adults (Reagh and Yassa, 2014; Reagh et al., 2016, 2018). The task, which is modeled after work in rodents, utilizes simple metric displacement to evaluate whether individuals can discriminate, across a delay, whether objects moved from their original locations. In this way, it is analogous to an object-location memory task but with distance varied being an operational metric to specifically test for spatial pattern separation deficits. Previous studies demonstrated that spatial pattern separation task performance in healthy older adults was not statistically different than that of young adults, despite deficits in the object domain (Reagh et al., 2018).

In this study of older adults with a range of cognitive performance (nondemented, but clinically impaired and unimpaired), we look beyond the hippocampus to formulate a mechanistic account for spatial pattern separation performance and use this to understand spatial memory deficits and their relationship to Alzheimer's pathology. These findings suggest that spatial memory deficits may arise due to changes in the functional connectivity of the PM network. While pattern separation is a computational process that is hypothesized to be supported by the hippocampus, specifically the DG, some studies have implicated regions beyond the hippocampus that are related to behavioral deficits in aging (Berron et al., 2018; Reagh et al., 2018). These results extend on this idea by demonstrating that the PM network, a network that is involved in processing of spatial information, helps support pattern separation. Here, we highlight that functional connectivity across regions in the PM network is strongly associated with out-of-scanner performance on the task, consistent with our hypothesis.

Here we find that the relationship between spatial pattern separation performance and verbal list recall (a standard test of hippocampal integrity) is contingent upon CSF levels of Aβ42/40, a hallmark pathology of Alzheimer's disease. Spatial pattern separation performance was also inversely correlated with CSF tau levels, consistent with AD-related impairment. These findings would suggest that spatial memory is affected by Alzheimer's disease pathology. However, it is unclear whether tau and Aβ deposition are driven by an upstream regulator.

Spatial memory dysfunction and cognitive decline

Determining how PMAT networks are altered in aging alone versus Alzheimer's disease may help in developing therapeutic targets to alleviate symptoms and potentially shift the PM network back to a normal state. In a recent randomized clinical trial with antiseizure drug levetiracetam (LEV), the study shows improved performance on spatial memory and executive function tasks in patients with Alzheimer's disease with subclinical epileptiform activity, which account for an estimated 60 percent of cases (Vossel et al., 2021). The study concludes that additional neuropsychological measures of network hyperexcitability are needed to determine the effects of antiseizure drugs on network dysfunction in patients with AD.

Our results show that performance on the spatial pattern separation task was predictive of longitudinal cognitive decline over a 1-2 year period (measured via the Mini-Mental State Exam). This would suggest that the spatial pattern separation task is a computerized assessment that can potentially serve as a "digital biomarker" by probing subtle features of cognitive decline during the earliest stages of the disease. While the task is a highly controlled version of what one would experience, and it is not a naturalistic environment, we would encounter similar experiences in our everyday lives. For example, older adults may have a difficult time

remembering where they parked their car or where they put their keys. These experiences would have overlapping representations since they contain information that is highly similar.

Overall, our results strongly suggest that spatial pattern separation may be a novel candidate for a digital biomarker that is mechanistically validated and predictive of cognitive decline.

Future Directions

Retroactive interference

While previous studies have reported relationships between pattern separation tasks and word list delayed recall (Reagh et al., 2014; Roberts et al., 2014), our studies show that retroactive interference is potentially driving this relationship. Future studies should examine retroactive interference as an early indicator of memory dysfunction.

Vascular and immune contributions

Our results show that dysfunction of the PM network and Alzheimer's disease pathology might underlie deficits in spatial pattern separation. However, it is unclear how network dysfunction and pathological changes are related. Novel candidates for elucidating whether upstream regulators are mediating or moderating this effect include inflammatory and neurovascular biomarkers. Future work should examine how inflammatory, and vascular indicators interact with established indicators such as amyloid and tau.

Regionally specific effects of AD pathology

One of the limitations in these experiments is that CSF biomarkers does not allow us to examine network specific burden. *In vivo* detection of amyloid pathology is possible with PET utilizing

amyloid-specific radiotracers. These tracers are Food and Drug Administration (FDA) approved and routinely being used to detect amyloid in the brains of patients with mild cognitive impairment (MCI) and AD. Numerous small-molecule PET tracers suitable for measuring Aβ in the living human brain have been developed over the past decade. Three of those tracers have been approved to interrogate brain Aβ plaque burden in suspected AD patients. One of those tracers is [^{18}F]AV-45 Florbetapir to screen for amyloid positivity.

PET tracers designed to interrogate NFT burden are under development as a complement to PET assessment of Aβ-burden at a pre-symptomatic stage of disease. In addition, a quantifiable biomarker of *in vivo* NFT pathology burden is of great interest as a tool to interrogate disease status with direct relevance to target pathology and clinical outcomes to support clinical evaluation of novel therapies for AD or other tauopathies. One of the limitations in the development of NFT PET tracers preventing the smooth translation of these tracers into clinical imaging studies is that NFT pathology and pattern of spread found in AD brain cannot be replicated in an animal model of disease. This inability to image pathological NFT burden using PET in animal models removes a valuable screening tool for tracer development and hampers the ability to translate imaging techniques directly from preclinical to clinical evaluation. Consequently, *in vivo* preclinical imaging signals are not possible and human studies are required to validate the utility of tau tracers. Several putative NFT imaging agents have been undergoing testing including [^{18}F]T-807 (Avid/Lilly), GTP-1 (Genentech), and several compounds developed by Tohoku university, such as [^{18}F]THK-5117 or [^{18}F]THK-5351 (GE Healthcare). Of these, [^{18}F]T-807 is the most extensively characterized having been studied in several hundred subjects. These PET tracers have all been generally well tolerated in early clinical studies (Villemagne et al., 2015; Xia et al., 2013). These ligands show increased tracer uptake and retention in brain regions generally consistent with

known distribution of NFT pathology in AD brains (i.e. the MTL). Furthermore, [^{18}F]T-807 PET imaging has also demonstrated increased uptake and signal retention in patients with prodromal AD (*i.e.*, mild cognitive impairment) (Villemagne et al., 2015). It has also demonstrated its capacity to detect Braak-stage specific tau binding (Schöll et al., 2015), as well as specificity of regional retention in the MTL to memory and hippocampal/entorhinal volume and cortical thickness.

The new [^{18}F]MK-6240 tracer (Merck) showed impressive results in early testing (Hostetler et al., 2016). Its binding pattern *in vitro* was consistent with the distribution of phosphorylated tau in human AD brain slices. It bound with high affinity to AD brain homogenates rich in NFTs but bound poorly to amyloid-plaque rich, NFT-poor AD brain homogenates. PET studies in monkeys showed rapid and homogeneous distribution, indicating favorable tracer kinetics. Importantly, MK-6240 does not appear to suffer from the off-target binding issues (Hostetler et al., 2016).

Community-based samples of ethnically diverse populations

Currently in the United States, Latinos or Hispanics are the second largest racial or ethnic group accounting for 18.5% of the population, and Black or African Americans are the third largest racial or ethnic group accounting for 13.4% of the population (US Census Bureau, 2020). Latinos or Hispanics and Black or African Americans are also disproportionately affected by Alzheimer's disease-related dementia (ADRD; Matthews et al., 2019; Mayeda et al., 2016; Tang et al., 2001). However, they are both underrepresented in observational and clinical studies, which limits the generalizability of many findings (McGarry and McColley, 2016).

Latinos or Hispanics, the largest and fastest growing minority in the United States, are an admixed group that includes White, Native American, and African ancestry (Hanis et al., 1991).

By 2060, the number of Latinos age 65 and older is expected to nearly quadruple, and Latinos are projected to have the largest increase in ADRD cases of any racial/ethnic group in the United States (Matthews et al., 2019). In the United States, the Food and Drug Administration (FDA) recently approved Aduhelm (aducanumab) for the treatment of Alzheimer's disease. Two double-blind, randomized, placebo-controlled dose-ranging studies were conducted: EMERGE and ENGAGE. However, in the EMERGE drug trial, out of 1638 participants, 4.1% were Latino or Hispanic, 0.7% were Black or African American, and 0.1% were American Indian or Alaskan Native (Biogen, 2021a). In the ENGAGE drug trial, out of 1647 participants, 2.2% were Latino or Hispanic, and 0.5% were Black or African American (Biogen, 2021b). Furthermore, the most common adverse events of the Aduhelm studies were due to cerebrovascular complications such as microhemorrhages and Amyloid-Related Imaging Abnormalities – Edema (ARIA-E). This may be of concern for Latinos since Latinos also face a high prevalence of cerebrovascular disease and higher prevalence of mixed pathologies (Filshtein et al., 2019). Risk factors that may contribute to the higher incidence of cerebrovascular disease include a higher prevalence of diabetes, cardiovascular disease, high blood pressure, obesity, and sleep apnea (Redline et al., 2014).

In California, Latinos or Hispanics are the largest racial or ethnic group accounting for 39.4% of the population, and in Orange County they are the largest minority accounting for 34.1% of the population (US Census Bureau, 2020). One of the limitations in our study is that the lack of racial and ethnic diversity in our sample, consisting of predominantly white individuals, thus limiting the generalizability of results. Future work should attempt to reproduce these findings in community-based samples drawn from ethnically diverse populations. One advantage with the spatial pattern separation task is that whereas auditory verbal learning tasks are dependent on

language, the spatial pattern separation task is not, potentially allowing for it to be easily adaptable.

REFERENCES

Alcolea, D., Pegueroles, J., Muñoz, L., Camacho, V., López-Mora, D., Fernández-León, A., Bastard, N.L., Huyck, E., Nadal, A., Olmedo, V., et al. (2019). Agreement of amyloid PET and CSF biomarkers for Alzheimer's disease on Lumipulse. Ann. Clin. Transl. Neurol. *6*, 1815–1824.

Allison, S.L., Fagan, A.M., Morris, J.C., and Head, D. (2016). Spatial Navigation in Preclinical Alzheimer's Disease. J. Alzheimers Dis. JAD *52*, 77–90.

Andersson, C., Lindau, M., Almkvist, O., Engfeldt, P., Johansson, S.-E., and Eriksdotter Jonhagen, M. (2006). Identifying patients at high and low risk of cognitive decline using Rey Auditory Verbal Learning Test among middle-aged memory clinic outpatients. Dement. Geriatr. Cogn. Disord. *21*, 251–259.

Avants, B., Duda, J.T., Kim, J., Zhang, H., Pluta, J., Gee, J.C., and Whyte, J. (2008). Multivariate analysis of structural and diffusion imaging in traumatic brain injury. Acad. Radiol. *15*, 1360–1375.

Bakker, A., Krauss, G.L., Albert, M.S., Speck, C.L., Jones, L.R., Stark, C.E., Yassa, M.A., Bassett, S.S., Shelton, A.L., and Gallagher, M. (2012). Reduction of Hippocampal Hyperactivity Improves Cognition in Amnestic Mild Cognitive Impairment. Neuron *74*, 467–474.

Balthazar, M.L.F., Yasuda, C.L., Cendes, F., and Damasceno, B.P. (2010). Learning, retrieval, and recognition are compromised in aMCI and mild AD: are distinct episodic memory processes mediated by the same anatomical structures? J. Int. Neuropsychol. Soc. JINS *16*, 205–209.

Bateman, R.J., Xiong, C., Benzinger, T.L.S., Fagan, A.M., Goate, A., Fox, N.C., Marcus, D.S., Cairns, N.J., Xie, X., Blazey, T.M., et al. (2012). Clinical and biomarker changes in dominantly inherited Alzheimer's disease. N. Engl. J. Med. *367*, 795–804.

Bayart, J.-L., Hanseeuw, B., Ivanoiu, A., and van Pesch, V. (2019). Analytical and clinical performances of the automated Lumipulse cerebrospinal fluid Aβ42 and T-Tau assays for Alzheimer's disease diagnosis. J. Neurol. *266*, 2304–2311.

Berron, D., Neumann, K., Maass, A., Schütze, H., Fliessbach, K., Kiven, V., Jessen, F., Sauvage, M., Kumaran, D., and Düzel, E. (2018). Age-related functional changes in domain-specific medial temporal lobe pathways. Neurobiol. Aging *65*, 86–97.

Biogen (2021a). (EMERGE) A Phase 3 Multicenter, Randomized, Double-Blind, Placebo-Controlled, Parallel-Group Study to Evaluate the Efficacy and Safety of Aducanumab (BIIB037) in Subjects With Early Alzheimer's Disease (clinicaltrials.gov).

Biogen (2021b). (ENGAGE) A Phase 3 Multicenter, Randomized, Double-Blind, Placebo-Controlled, Parallel-Group Study to Evaluate the Efficacy and Safety of Aducanumab (BIIB037) in Subjects With Early Alzheimer's Disease (clinicaltrials.gov).

Biswal, B., Yetkin, F.Z., Haughton, V.M., and Hyde, J.S. (1995). Functional connectivity in the motor cortex of resting human brain using echo-planar MRI. Magn. Reson. Med. Off. J. Soc. Magn. Reson. Med. Soc. Magn. Reson. Med. *34*, 537–541.

Blennow, K., Hampel, H., Weiner, M., and Zetterberg, H. (2010). Cerebrospinal fluid and plasma biomarkers in Alzheimer disease. Nat. Rev. Neurol. *6*, 131–144.

Braak, H., and Braak, E. (1991). Neuropathological stageing of Alzheimer-related changes. Acta Neuropathol. (Berl.) *82*, 239–259.

Braak, H., and Braak, E. (1999). Temporal Sequence of Alzheimer's Disease-Related Pathology. In Cerebral Cortex: Neurodegenerative and Age-Related Changes in Structure and Function of Cerebral Cortex, A. Peters, and J.H. Morrison, eds. (Boston, MA: Springer US), pp. 475–512.

Braak, H., and Del Tredici, K. (2011). The pathological process underlying Alzheimer's disease in individuals under thirty. Acta Neuropathol. (Berl.) *121*, 171–181.

Braak, H., and Tredici, K.D. (2015). Neuroanatomy and Pathology of Sporadic Alzheimer's Disease (Springer International Publishing).

Buckner, R.L., Andrews-Hanna, J.R., and Schacter, D.L. (2008). The brain's default network: anatomy, function, and relevance to disease. Ann. N. Y. Acad. Sci. *1124*, 1–38.

Burles, F., Slone, E., and Iaria, G. (2017). Dorso-medial and ventro-lateral functional specialization of the human retrosplenial complex in spatial updating and orienting. Brain Struct. Funct. *222*, 1481–1493.

Burwell, R.D., and Amaral, D.G. (1998). Cortical afferents of the perirhinal, postrhinal, and entorhinal cortices of the rat. J. Comp. Neurol. *398*, 179–205.

Campbell, M.R., Ashrafzadeh-Kian, S., Petersen, R.C., Mielke, M.M., Syrjanen, J.A., Harten, A.C. van, Lowe, V.J., Jack, C.R., Bornhorst, J.A., and Algeciras-Schimnich, A. (2021). P-

tau/Aβ42 and Aβ42/40 ratios in CSF are equally predictive of amyloid PET status. Alzheimers Dement. Diagn. Assess. Dis. Monit. *13*, e12190.

Cox, R.W. (1996). AFNI: software for analysis and visualization of functional magnetic resonance neuroimages. Comput. Biomed. Res. Int. J. *29*, 162–173.

Craft, S., Newcomer, J., Kanne, S., Dagogo-Jack, S., Cryer, P., Sheline, Y., Luby, J., Dagogo-Jack, A., and Alderson, A. (1996). Memory improvement following induced hyperinsulinemia in alzheimer's disease. Neurobiol. Aging *17*, 123–130.

Crary, J.F., Trojanowski, J.Q., Schneider, J.A., Abisambra, J.F., Abner, E.L., Alafuzoff, I., Arnold, S.E., Attems, J., Beach, T.G., Bigio, E.H., et al. (2014). Primary age-related tauopathy (PART): a common pathology associated with human aging. Acta Neuropathol. (Berl.) *128*, 755–766.

Crocco, E., Curiel, R.E., Acevedo, A., Czaja, S.J., and Loewenstein, D.A. (2014). An Evaluation of Deficits in Semantic Cuing, Proactive and Retroactive Interference as Early Features of Alzheimer's disease. Am. J. Geriatr. Psychiatry Off. J. Am. Assoc. Geriatr. Psychiatry *22*, 889–897.

Dale, A.M., Fischl, B., and Sereno, M.I. (1999). Cortical surface-based analysis. I. Segmentation and surface reconstruction. NeuroImage *9*, 179–194.

Deshmukh, S.S., and Knierim, J.J. (2011). Representation of non-spatial and spatial information in the lateral entorhinal cortex. Front. Behav. Neurosci. *5*, 69.

Dickerson, B.C., and Eichenbaum, H. (2010). The episodic memory system: neurocircuitry and disorders. Neuropsychopharmacol. Off. Publ. Am. Coll. Neuropsychopharmacol. *35*, 86–104.

Dickerson, B.C., Salat, D.H., Bates, J.F., Atiya, M., Killiany, R.J., Greve, D.N., Dale, A.M., Stern, C.E., Blacker, D., Albert, M.S., et al. (2004). Medial temporal lobe function and structure in mild cognitive impairment. Ann. Neurol. *56*, 27–35.

Dickerson, B.C., Salat, D.H., Greve, D.N., Chua, E.F., Rand-Giovannetti, E., Rentz, D.M., Bertram, L., Mullin, K., Tanzi, R.E., Blacker, D., et al. (2005). Increased hippocampal activation in mild cognitive impairment compared to normal aging and AD. Neurology *65*, 404–411.

Doeller, C.F., Barry, C., and Burgess, N. (2010a). Evidence for grid cells in a human memory network. Nature *463*, 657–661.

Doeller, C.F., Barry, C., and Burgess, N. (2010b). Evidence for grid cells in a human memory network. Nature *463*, 657–661.

Dubois, B., Feldman, H.H., Jacova, C., Hampel, H., Molinuevo, J.L., Blennow, K., DeKosky, S.T., Gauthier, S., Selkoe, D., Bateman, R., et al. (2014). Advancing research diagnostic criteria for Alzheimer's disease: the IWG-2 criteria. Lancet Neurol. *13*, 614–629.

Duyckaerts, C., and Hauw, J.J. (1997). Prevalence, incidence and duration of Braak's stages in the general population: can we know? Neurobiol. Aging *18*, 362–369; discussion 389-392.

Duyckaerts, C., Braak, H., Brion, J.-P., Buée, L., Del Tredici, K., Goedert, M., Halliday, G., Neumann, M., Spillantini, M.G., Tolnay, M., et al. (2015). PART is part of Alzheimer disease. Acta Neuropathol. (Berl.) *129*, 749–756.

Eichenbaum, H., Yonelinas, A.P., and Ranganath, C. (2007). The medial temporal lobe and recognition memory. Annu. Rev. Neurosci. *30*, 123–152.

Ekstrom, A.D., Kahana, M.J., Caplan, J.B., Fields, T.A., Isham, E.A., Newman, E.L., and Fried, I. (2003). Cellular networks underlying human spatial navigation. Nature *425*, 184–188.

Elman, J.A., Oh, H., Madison, C.M., Baker, S.L., Vogel, J.W., Marks, S.M., Crowley, S., O'Neil, J.P., and Jagust, W.J. (2014). Neural compensation in older people with brain amyloid-β deposition. Nat. Neurosci. *17*, 1316–1318.

Estévez-González, A., Kulisevsky, J., Boltes, A., Otermín, P., and García-Sánchez, C. (2003). Rey verbal learning test is a useful tool for differential diagnosis in the preclinical phase of Alzheimer's disease: comparison with mild cognitive impairment and normal aging. Int. J. Geriatr. Psychiatry *18*, 1021–1028.

Ewers, M., Sperling, R.A., Klunk, W.E., Weiner, M.W., and Hampel, H. (2011). Neuroimaging markers for the prediction and early diagnosis of Alzheimer's disease dementia. Trends Neurosci. *34*, 430–442.

Filshtein, T.J., Dugger, B.N., Jin, L.-W., Olichney, J.M., Farias, S.T., Carvajal-Carmona, L., Lott, P., Mungas, D., Reed, B., Beckett, L.A., et al. (2019). Neuropathological Diagnoses of Demented Hispanic, Black, and Non-Hispanic White Decedents Seen at an Alzheimer's Disease Center. J. Alzheimers Dis. *68*, 145–158.

Fischl, B., Sereno, M.I., and Dale, A.M. (1999). Cortical surface-based analysis. II: Inflation, flattening, and a surface-based coordinate system. NeuroImage *9*, 195–207.

Fox, M.D., and Raichle, M.E. (2007). Spontaneous fluctuations in brain activity observed with functional magnetic resonance imaging. Nat Rev Neurosci *8*, 700–711.

Fredericks, C.A., Sturm, V.E., Brown, J.A., Hua, A.Y., Bilgel, M., Wong, D.F., Resnick, S.M., and Seeley, W.W. (2018). Early affective changes and increased connectivity in preclinical Alzheimer's disease. Alzheimers Dement. Diagn. Assess. Dis. Monit. *10*, 471–479.

Fyhn, M., Molden, S., Witter, M.P., Moser, E.I., and Moser, M.-B. (2004). Spatial Representation in the Entorhinal Cortex. Science *305*, 1258–1264.

Gilbert, P.E., Kesner, R.P., and DeCoteau, W.E. (1998). Memory for spatial location: role of the hippocampus in mediating spatial pattern separation. J. Neurosci. Off. J. Soc. Neurosci. *18*, 804–810.

Greicius, M.D., and Menon, V. (2004). Default-mode activity during a passive sensory task: uncoupled from deactivation but impacting activation. J. Cogn. Neurosci. *16*, 1484–1492.

Gusnard, D.A., and Raichle, M.E. (2001). Searching for a baseline: Functional imaging and the resting human brain. Nat. Rev. Neurosci. *2*, 685–694.

Hafting, T., Fyhn, M., Molden, S., Moser, M.-B., and Moser, E.I. (2005). Microstructure of a spatial map in the entorhinal cortex. Nature *436*, 801–806.

Hanis, C.L., Hewett-Emmett, D., Bertin, T.K., and Schull, W.J. (1991). Origins of U.S. Hispanics. Implications for diabetes. Diabetes Care *14*, 618–627.

Hansson, O., Seibyl, J., Stomrud, E., Zetterberg, H., Trojanowski, J.Q., Bittner, T., Lifke, V., Corradini, V., Eichenlaub, U., Batrla, R., et al. (2018). CSF biomarkers of Alzheimer's disease

concord with amyloid-β PET and predict clinical progression: A study of fully automated immunoassays in BioFINDER and ADNI cohorts. Alzheimers Dement. J. Alzheimers Assoc. *14*, 1470–1481.

Hof, P.R., Glannakopoulos, P., and Bouras, C. (1996). The neuropathological changes associated with normal brain aging. Histol. Histopathol. *11*, 1075–1088.

Holden, H.M., and Gilbert, P.E. (2012). Less efficient pattern separation may contribute to age-related spatial memory deficits. Front. Aging Neurosci. *4*.

Hope, T., Tilling, K.M., Gedling, K., Keene, J.M., Cooper, S.D., and Fairburn, C.G. (1994). The structure of wandering in dementia. Int. J. Geriatr. Psychiatry *9*, 149–155.

Hostetler, E.D., Walji, A.M., Zeng, Z., Miller, P., Bennacef, I., Salinas, C., Connolly, B., Gantert, L., Haley, H., Holahan, M., et al. (2016). Preclinical Characterization of 18F-MK-6240, a Promising PET Tracer for In Vivo Quantification of Human Neurofibrillary Tangles. J. Nucl. Med. Off. Publ. Soc. Nucl. Med. *57*, 1599–1606.

Høydal, Ø.A., Skytøen, E.R., Andersson, S.O., Moser, M.-B., and Moser, E.I. (2019). Object-vector coding in the medial entorhinal cortex. Nature *568*, 400–404.

Huijbers, W., Mormino, E.C., Wigman, S.E., Ward, A.M., Vannini, P., McLaren, D.G., Becker, J.A., Schultz, A.P., Hedden, T., Johnson, K.A., et al. (2014). Amyloid Deposition Is Linked to Aberrant Entorhinal Activity among Cognitively Normal Older Adults. J. Neurosci. *34*, 5200–5210.

Huijbers, W., Schultz, A.P., Papp, K.V., LaPoint, M.R., Hanseeuw, B., Chhatwal, J.P., Hedden, T., Johnson, K.A., and Sperling, R.A. (2019). Tau Accumulation in Clinically Normal Older Adults Is Associated with Hippocampal Hyperactivity. J. Neurosci. *39*, 548–556.

Inhoff, M.C., and Ranganath, C. (2017). Dynamic cortico-hippocampal networks underlying memory and cognition: The PMAT framework. In The Hippocampus from Cells to Systems: Structure, Connectivity, and Functional Contributions to Memory and Flexible Cognition, (Cham, Switzerland: Springer International Publishing), pp. 559–589.

Insausti, R., and Amaral, D.G. (2008). The Entorhinal Cortex of the Monkey: IV. Topographical and Laminar Organization of Cortical Afferents. J. Comp. Neurol. *509*, 608–641.

Insausti, R., Amaral, D.G., and Cowan, W.M. (1987). The entorhinal cortex of the monkey: II. Cortical afferents. J. Comp. Neurol. *264*, 356–395.

Jack, C.R., and Holtzman, D.M. (2013). Biomarker modeling of Alzheimer's disease. Neuron *80*, 1347–1358.

Jack, C.R., Bennett, D.A., Blennow, K., Carrillo, M.C., Feldman, H.H., Frisoni, G.B., Hampel, H., Jagust, W.J., Johnson, K.A., Knopman, D.S., et al. (2016). A/T/N: An unbiased descriptive classification scheme for Alzheimer disease biomarkers. Neurology *87*, 539–547.

Jack, C.R., Bennett, D.A., Blennow, K., Carrillo, M.C., Dunn, B., Haeberlein, S.B., Holtzman, D.M., Jagust, W., Jessen, F., Karlawish, J., et al. (2018). NIA-AA Research Framework: Toward a biological definition of Alzheimer's disease. Alzheimers Dement. J. Alzheimers Assoc. *14*, 535–562.

Jack Jr, C.R., Knopman, D.S., Jagust, W.J., Shaw, L.M., Aisen, P.S., Weiner, M.W., Petersen, R.C., and Trojanowski, J.Q. (2010). Hypothetical model of dynamic biomarkers of the Alzheimer's pathological cascade. Lancet Neurol. *9*, 119–128.

Jack Jr, C.R., Knopman, D.S., Jagust, W.J., Petersen, R.C., Weiner, M.W., Aisen, P.S., Shaw, L.M., Vemuri, P., Wiste, H.J., Weigand, S.D., et al. (2013). Tracking pathophysiological processes in Alzheimer's disease: an updated hypothetical model of dynamic biomarkers. Lancet Neurol. *12*, 207–216.

Jacobs, J., Weidemann, C.T., Miller, J.F., Solway, A., Burke, J.F., Wei, X.-X., Suthana, N., Sperling, M.R., Sharan, A.D., Fried, I., et al. (2013). Direct recordings of grid-like neuronal activity in human spatial navigation. Nat. Neurosci. *16*, 1188–1190.

Janelidze, S., Zetterberg, H., Mattsson, N., Palmqvist, S., Vanderstichele, H., Lindberg, O., van Westen, D., Stomrud, E., Minthon, L., Blennow, K., et al. (2016). CSF Aβ42/Aβ40 and Aβ42/Aβ38 ratios: better diagnostic markers of Alzheimer disease. Ann. Clin. Transl. Neurol. *3*, 154–165.

Janelidze, S., Pannee, J., Mikulskis, A., Chiao, P., Zetterberg, H., Blennow, K., and Hansson, O. (2017). Concordance Between Different Amyloid Immunoassays and Visual Amyloid Positron Emission Tomographic Assessment. JAMA Neurol. *74*, 1492–1501.

Jones, D.T., Knopman, D.S., Gunter, J.L., Graff-Radford, J., Vemuri, P., Boeve, B.F., Petersen, R.C., Weiner, M.W., Jack, C.R., and Alzheimer's Disease Neuroimaging Initiative (2016). Cascading network failure across the Alzheimer's disease spectrum. Brain J. Neurol. *139*, 547–562.

Jun, H., Bramian, A., Soma, S., Saito, T., Saido, T.C., and Igarashi, K.M. (2020). Disrupted Place Cell Remapping and Impaired Grid Cells in a Knockin Model of Alzheimer's Disease. Neuron *107*, 1095-1112.e6.

Killian, N.J., Jutras, M.J., and Buffalo, E.A. (2012). A map of visual space in the primate entorhinal cortex. Nature *491*, 761–764.

Klunk, W.E., Engler, H., Nordberg, A., Wang, Y., Blomqvist, G., Holt, D.P., Bergström, M., Savitcheva, I., Huang, G.-F., Estrada, S., et al. (2004). Imaging brain amyloid in Alzheimer's disease with Pittsburgh Compound-B. Ann. Neurol. *55*, 306–319.

Kobayashi, Y., and Amaral, D.G. (2003). Macaque monkey retrosplenial cortex: II. Cortical afferents. J. Comp. Neurol. *466*, 48–79.

Koychev, I., Hofer, M., and Friedman, N. (2020). Correlation of Alzheimer Disease Neuropathologic Staging with Amyloid and Tau Scintigraphic Imaging Biomarkers. J. Nucl. Med. *61*, 1413–1418.

Kuhl, B.A., Shah, A.T., DuBrow, S., and Wagner, A.D. (2010). Resistance to forgetting associated with hippocampus-mediated reactivation during new learning. Nat. Neurosci. *13*, 501–506.

Kunz, L., Schröder, T.N., Lee, H., Montag, C., Lachmann, B., Sariyska, R., Reuter, M., Stirnberg, R., Stöcker, T., Messing-Floeter, P.C., et al. (2015). Reduced grid-cell-like representations in adults at genetic risk for Alzheimer's disease. Science *350*, 430–433.

Landau, S.M., Mintun, M.A., Joshi, A.D., Koeppe, R.A., Petersen, R.C., Aisen, P.S., Weiner, M.W., Jagust, W.J., and Alzheimer's Disease Neuroimaging Initiative (2012). Amyloid deposition, hypometabolism, and longitudinal cognitive decline. Ann. Neurol. *72*, 578–586.

Landau, S.M., Breault, C., Joshi, A.D., Pontecorvo, M., Mathis, C.A., Jagust, W.J., Mintun, M.A., and Alzheimer's Disease Neuroimaging Initiative (2013). Amyloid-β imaging with Pittsburgh compound B and florbetapir: comparing radiotracers and quantification methods. J. Nucl. Med. Off. Publ. Soc. Nucl. Med. *54*, 70–77.

Leal, S.L., and Yassa, M. a. (2013). Perturbations of neural circuitry in aging, mild cognitive impairment, and Alzheimer's disease. Ageing Res. Rev. *12*, 823–831.

Leal, S.L., and Yassa, M.A. (2015). Neurocognitive Aging and the Hippocampus Across Species. Trends Neurosci. *38*, 800–812.

Leal, S.L., and Yassa, M.A. (2018). Integrating new findings and examining clinical applications of pattern separation. Nat. Neurosci. *21*, 163–173.

Leal, S.L., Landau, S.M., Bell, R.K., and Jagust, W.J. (2017). Hippocampal activation is associated with longitudinal amyloid accumulation and cognitive decline. ELife *6*.

Leal, S.L., Lockhart, S.N., Maass, A., Bell, R.K., and Jagust, W.J. (2018). Subthreshold Amyloid Predicts Tau Deposition in Aging. J. Neurosci. *38*, 4482–4489.

Lewczuk, P., Matzen, A., Blennow, K., Parnetti, L., Molinuevo, J.L., Eusebi, P., Kornhuber, J., Morris, J.C., and Fagan, A.M. (2017). Cerebrospinal Fluid Aβ42/40 Corresponds Better than Aβ42 to Amyloid PET in Alzheimer's Disease. J. Alzheimers Dis. JAD *55*, 813–822.

Lithfous, S., Dufour, A., and Després, O. (2013). Spatial navigation in normal aging and the prodromal stage of Alzheimer's disease: insights from imaging and behavioral studies. Ageing Res. Rev. *12*, 201–213.

Lockhart, S.N., Schöll, M., Baker, S.L., Ayakta, N., Swinnerton, K.N., Bell, R.K., Mellinger, T.J., Shah, V.D., O'Neil, J.P., Janabi, M., et al. (2017). Amyloid and tau PET demonstrate region-specific associations in normal older people. NeuroImage *150*, 191–199.

Loewenstein, D.A., Acevedo, A., Luis, C., Crum, T., Barker, W.W., and Duara, R. (2004). Semantic interference deficits and the detection of mild Alzheimer's disease and mild cognitive impairment without dementia. J. Int. Neuropsychol. Soc. JINS *10*, 91–100.

Maass, A., Berron, D., Libby, L.A., Ranganath, C., and Düzel, E. (2015). Functional subregions of the human entorhinal cortex.

Maass, A., Lockhart, S.N., Harrison, T.M., Bell, R.K., Mellinger, T., Swinnerton, K., Baker, S.L., Rabinovici, G.D., and Jagust, W.J. (2018). Entorhinal Tau Pathology, Episodic Memory Decline, and Neurodegeneration in Aging. J. Neurosci. Off. J. Soc. Neurosci. *38*, 530–543.

Maass, A., Berron, D., Harrison, T.M., Adams, J.N., La Joie, R., Baker, S., Mellinger, T., Bell, R.K., Swinnerton, K., Inglis, B., et al. (2019). Alzheimer's pathology targets distinct memory networks in the ageing brain. Brain J. Neurol. *142*, 2492–2509.

Marks, S.M., Lockhart, S.N., Baker, S.L., and Jagust, W.J. (2017). Tau and β-Amyloid Are Associated with Medial Temporal Lobe Structure, Function, and Memory Encoding in Normal Aging. J. Neurosci. *37*, 3192–3201.

Márquez, F., and Yassa, M.A. (2019). Neuroimaging Biomarkers for Alzheimer's Disease. Mol. Neurodegener. *14*, 21.

Marr, D. (1971). Simple memory: a theory for archicortex. Philos. Trans. R. Soc. Lond. B. Biol. Sci. *262*, 23–81.

Matthews, K.A., Xu, W., Gaglioti, A.H., Holt, J.B., Croft, J.B., Mack, D., and McGuire, L.C. (2019). Racial and ethnic estimates of Alzheimer's disease and related dementias in the United States (2015-2060) in adults aged ≥65 years. Alzheimers Dement. J. Alzheimers Assoc. *15*, 17–24.

Mayeda, E.R., Glymour, M.M., Quesenberry, C.P., and Whitmer, R.A. (2016). Inequalities in dementia incidence between six racial and ethnic groups over 14 years. Alzheimers Dement. J. Alzheimers Assoc. *12*, 216–224.

McClelland, J.L., McNaughton, B.L., and O'Reilly, R.C. (1995). Why there are complementary learning systems in the hippocampus and neocortex: Insights from the successes and failures of connectionist models of learning and memory. Psychol. Rev. *102*, 419–457.

McGarry, M.E., and McColley, S.A. (2016). Minorities Are Underrepresented in Clinical Trials of Pharmaceutical Agents for Cystic Fibrosis. Ann. Am. Thorac. Soc. *13*, 1721–1725.

McKhann, G.M., Knopman, D.S., Chertkow, H., Hyman, B.T., Jack, C.R., Kawas, C.H., Klunk, W.E., Koroshetz, W.J., Manly, J.J., Mayeux, R., et al. (2011). The diagnosis of dementia due to Alzheimer's disease: Recommendations from the National Institute on Aging-Alzheimer's Association workgroups on diagnostic guidelines for Alzheimer's disease. Alzheimers Dement. *7*, 263–269.

Miao, C., Cao, Q., Moser, M.-B., and Moser, E.I. (2017). Parvalbumin and Somatostatin Interneurons Control Different Space-Coding Networks in the Medial Entorhinal Cortex. Cell *171*, 507-521.e17.

Miller, S.L., Fenstermacher, E., Bates, J., Blacker, D., Sperling, R.A., and Dickerson, B.C. (2008a). Hippocampal activation in adults with mild cognitive impairment predicts subsequent cognitive decline. J. Neurol. Neurosurg. Psychiatry *79*, 630–635.

Miller, S.L., Celone, K., DePeau, K., Diamond, E., Dickerson, B.C., Rentz, D., Pihlajamäki, M., and Sperling, R.A. (2008b). Age-related memory impairment associated with loss of parietal deactivation but preserved hippocampal activation. Proc. Natl. Acad. Sci. *105*, 2181–2186.

Milner, B., Squire, L.R., and Kandel, E.R. (1998). Cognitive neuroscience and the study of memory. Neuron *20*, 445–468.

Montchal, M.E., Reagh, Z.M., and Yassa, M.A. (2019). Precise temporal memories are supported by the lateral entorhinal cortex in humans. Nat. Neurosci. *22*, 284–288.

Moradi, E., Pepe, A., Gaser, C., Huttunen, H., and Tohka, J. (2015). Machine learning framework for early MRI-based Alzheimer's conversion prediction in MCI subjects. NeuroImage *104*, 398–412.

Moradi, E., Hallikainen, I., Hänninen, T., Tohka, J., and Alzheimer's Disease Neuroimaging Initiative (2017). Rey's Auditory Verbal Learning Test scores can be predicted from whole brain MRI in Alzheimer's disease. NeuroImage Clin. *13*, 415–427.

Mormino, E.C., Brandel, M.G., Madison, C.M., Marks, S., Baker, S.L., and Jagust, W.J. (2012). Aβ Deposition in Aging Is Associated with Increases in Brain Activation during Successful Memory Encoding. Cereb. Cortex N. Y. NY *22*, 1813–1823.

Morris, R.G.M., Garrud, P., Rawlins, J.N.P., and O'Keefe, J. (1982). Place navigation impaired in rats with hippocampal lesions. Nature *297*, 681–683.

Naber, P.A., Caballero-Bleda, M., Jorritsma-Byham, B., and Witter, M.P. (1997). Parallel input to the hippocampal memory system through peri- and postrhinal cortices. Neuroreport *8*, 2617–2621.

Nasreddine, Z.S., Phillips, N.A., Bédirian, V., Charbonneau, S., Whitehead, V., Collin, I., Cummings, J.L., and Chertkow, H. (2005). The Montreal Cognitive Assessment, MoCA: A Brief Screening Tool For Mild Cognitive Impairment. J. Am. Geriatr. Soc. *53*, 695–699.

Navarro Schröder, T., Haak, K.V., Zaragoza Jimenez, N.I., Beckmann, C.F., and Doeller, C.F. (2015). Functional topography of the human entorhinal cortex. ELife *4*, e06738.

Öhman, F., Hassenstab, J., Berron, D., Schöll, M., and Papp, K.V. (2021). Current advances in digital cognitive assessment for preclinical Alzheimer's disease. Alzheimers Dement. Diagn. Assess. Dis. Monit. *13*, e12217.

O'Keefe, J., and Dostrovsky, J. (1971). The hippocampus as a spatial map: Preliminary evidence from unit activity in the freely-moving rat. Brain Res. *34*, 171–175.

Palmqvist, S., Mattsson, N., Hansson, O., and Alzheimer's Disease Neuroimaging Initiative (2016). Cerebrospinal fluid analysis detects cerebral amyloid-β accumulation earlier than positron emission tomography. Brain J. Neurol. *139*, 1226–1236.

Palmqvist, S., Schöll, M., Strandberg, O., Mattsson, N., Stomrud, E., Zetterberg, H., Blennow, K., Landau, S., Jagust, W., and Hansson, O. (2017). Earliest accumulation of β-amyloid occurs within the default-mode network and concurrently affects brain connectivity. Nat. Commun. *8*, 1214.

Papp, K.V., Rentz, D.M., Maruff, P., Sun, C.-K., Raman, R., Donohue, M.C., Schembri, A., Stark, C., Yassa, M.A., Wessels, A.M., et al. (2021). The Computerized Cognitive Composite (C3) in A4, an Alzheimer's Disease Secondary Prevention Trial. J. Prev. Alzheimers Dis. *8*, 59–67.

Perl, D.P. (2010). Neuropathology of Alzheimer's disease. Mt. Sinai J. Med. N. Y. *77*, 32–42.

Petrella, J.R., Sheldon, F.C., Prince, S.E., Calhoun, V.D., and Doraiswamy, P.M. (2011). Default mode network connectivity in stable vs progressive mild cognitive impairment. Neurology *76*, 511–517.

Possin, K.L., Laluz, V.R., Alcantar, O.Z., Miller, B.L., and Kramer, J.H. (2011). Distinct neuroanatomical substrates and cognitive mechanisms of figure copy performance in Alzheimer's disease and behavioral variant frontotemporal dementia. Neuropsychologia *49*, 43–48.

Putcha, D., Brickhouse, M., O'Keefe, K., Sullivan, C., Rentz, D., Marshall, G., Dickerson, B., and Sperling, R. (2011). Hippocampal Hyperactivation Associated with Cortical Thinning in

Alzheimer's Disease Signature Regions in Non-Demented Elderly Adults. J. Neurosci. *31*, 17680–17688.

Raichle, M.E., MacLeod, A.M., Snyder, A.Z., Powers, W.J., Gusnard, D.A., and Shulman, G.L. (2001). A default mode of brain function. Proc. Natl. Acad. Sci. *98*, 676–682.

Ranganath, C., and Ritchey, M. (2012). Two cortical systems for memory-guided behaviour. Nat. Rev. Neurosci. *13*, 713–726.

Reagh, Z.M., and Yassa, M.A. (2014). Object and spatial mnemonic interference differentially engage lateral and medial entorhinal cortex in humans. Proc. Natl. Acad. Sci. 201411250.

Reagh, Z.M., Roberts, J.M., Ly, M., DiProspero, N., Murray, E., and Yassa, M.A. (2014). Spatial discrimination deficits as a function of mnemonic interference in aged adults with and without memory impairment. Hippocampus *24*, 303–314.

Reagh, Z.M., Ho, H.D., Leal, S.L., Noche, J.A., Chun, A., Murray, E.A., and Yassa, M.A. (2016). Greater loss of object than spatial mnemonic discrimination in aged adults. Hippocampus *26*, 417–422.

Reagh, Z.M., Noche, J.A., Tustison, N.J., Delisle, D., Murray, E.A., and Yassa, M.A. (2018). Functional Imbalance of Anterolateral Entorhinal Cortex and Hippocampal Dentate/CA3 Underlies Age-Related Object Pattern Separation Deficits. Neuron *97*, 1187-1198.e4.

Redline, S., Sotres-Alvarez, D., Loredo, J., Hall, M., Patel, S.R., Ramos, A., Shah, N., Ries, A., Arens, R., Barnhart, J., et al. (2014). Sleep-disordered Breathing in Hispanic/Latino Individuals

of Diverse Backgrounds. The Hispanic Community Health Study/Study of Latinos. Am. J. Respir. Crit. Care Med. *189*, 335–344.

Reitan, R.M., and Wolfson, D. (1985). The Halstead-Reitan neuropsychological test battery: Theory and clinical interpretation (Reitan Neuropsychology).

Ritchey, M., Yonelinas, A.P., and Ranganath, C. (2014). Functional connectivity relationships predict similarities in task activation and pattern information during associative memory encoding. J. Cogn. Neurosci. *26*, 1085–1099.

Ritchey, M., Libby, L.A., and Ranganath, C. (2015). Cortico-hippocampal systems involved in memory and cognition: the PMAT framework. Prog. Brain Res. *219*, 45–64.

Roberts, J.M., Ly, M., Murray, E., and Yassa, M.A. (2014). Temporal discrimination deficits as a function of lag interference in older adults. Hippocampus *24*, 1189–1196.

Rodo, C., Sargolini, F., and Save, E. (2017). Processing of spatial and non-spatial information in rats with lesions of the medial and lateral entorhinal cortex: Environmental complexity matters. Behav. Brain Res. *320*, 200–209.

Sanz-Arigita, E.J., Schoonheim, M.M., Damoiseaux, J.S., Rombouts, S.A.R.B., Maris, E., Barkhof, F., Scheltens, P., and Stam, C.J. (2010). Loss of "small-world" networks in Alzheimer's disease: graph analysis of FMRI resting-state functional connectivity. PloS One *5*, e13788.

Sargolini, F., Fyhn, M., Hafting, T., McNaughton, B.L., Witter, M.P., Moser, M.-B., and Moser, E.I. (2006). Conjunctive representation of position, direction, and velocity in entorhinal cortex. Science *312*, 758–762.

Schindler, S.E., Gray, J.D., Gordon, B.A., Xiong, C., Batrla-Utermann, R., Quan, M., Wahl, S., Benzinger, T.L.S., Holtzman, D.M., Morris, J.C., et al. (2018). Cerebrospinal fluid biomarkers measured by Elecsys assays compared to amyloid imaging. Alzheimers Dement. J. Alzheimers Assoc. *14*, 1460–1469.

Schöll, M., Schonhaut, D., Lockhart, S., Vogel, J.W., Baker, S., Schwimmer, H., Ossenkoppele, R., Rabinovici, G.D., and Jagust, W.J. (2015). In vivo braak staging using 18F-AV1451 Tau PET imaging. Alzheimers Dement. J. Alzheimers Assoc. *11*, P4.

Schultz, A.P., Chhatwal, J.P., Hedden, T., Mormino, E.C., Hanseeuw, B.J., Sepulcre, J., Huijbers, W., LaPoint, M., Buckley, R.F., Johnson, K.A., et al. (2017). Phases of Hyperconnectivity and Hypoconnectivity in the Default Mode and Salience Networks Track with Amyloid and Tau in Clinically Normal Individuals. J. Neurosci. *37*, 4323–4331.

Schultz, H., Sommer, T., and Peters, J. (2015). The Role of the Human Entorhinal Cortex in a Representational Account of Memory. Front. Hum. Neurosci. *9*.

Schwarz, A.J., Yu, P., Miller, B.B., Shcherbinin, S., Dickson, J., Navitsky, M., Joshi, A.D., Devous, M.D., Sr, and Mintun, M.S. (2016). Regional profiles of the candidate tau PET ligand 18 F-AV-1451 recapitulate key features of Braak histopathological stages. Brain *139*, 1539–1550.

Scoville, W.B., and Milner, B. (1957). LOSS OF RECENT MEMORY AFTER BILATERAL HIPPOCAMPAL LESIONS. J. Neurol. Neurosurg. Psychiatry *20*, 11–21.

Sepulcre, J., Schultz, A.P., Sabuncu, M., Gomez-Isla, T., Chhatwal, J., Becker, A., Sperling, R., and Johnson, K.A. (2016). In Vivo Tau, Amyloid, and Gray Matter Profiles in the Aging Brain. J. Neurosci. Off. J. Soc. Neurosci. *36*, 7364–7374.

Sheline, Y.I., and Raichle, M.E. (2013). Resting state functional connectivity in preclinical Alzheimer's disease. Biol. Psychiatry *74*, 340–347.

Sherrill, K.R., Erdem, U.M., Ross, R.S., Brown, T.I., Hasselmo, M.E., and Stern, C.E. (2013). Hippocampus and Retrosplenial Cortex Combine Path Integration Signals for Successful Navigation. J. Neurosci. *33*, 19304–19313.

Solstad, T., Boccara, C.N., Kropff, E., Moser, M.-B., and Moser, E.I. (2008). Representation of geometric borders in the entorhinal cortex. Science *322*, 1865–1868.

Sperling, R.A., Laviolette, P.S., O'Keefe, K., O'Brien, J., Rentz, D.M., Pihlajamaki, M., Marshall, G., Hyman, B.T., Selkoe, D.J., Hedden, T., et al. (2009). Amyloid deposition is associated with impaired default network function in older persons without dementia. Neuron *63*, 178–188.

Sperling, R.A., Aisen, P.S., Beckett, L.A., Bennett, D.A., Craft, S., Fagan, A.M., Iwatsubo, T., Jack Jr., C.R., Kaye, J., Montine, T.J., et al. (2011). Toward defining the preclinical stages of Alzheimer's disease: Recommendations from the National Institute on Aging-Alzheimer's Association workgroups on diagnostic guidelines for Alzheimer's disease. Alzheimers Dement. *7*, 280–292.

Squire, L.R., Stark, C.E.L., and Clark, R.E. (2004). The medial temporal lobe. Annu. Rev. Neurosci. *27*, 279–306.

Stark, S.M., Yassa, M.A., and Stark, C.E.L. (2010). Individual differences in spatial pattern separation performance associated with healthy aging in humans. Learn. Mem. *17*, 284–288.

Stark, S.M., Yassa, M.A., Lacy, J.W., and Stark, C.E.L. (2013). A task to assess behavioral pattern separation (BPS) in humans: Data from healthy aging and mild cognitive impairment. Neuropsychologia *51*, 2442–2449.

Steffenach, H.-A., Witter, M., Moser, M.-B., and Moser, E.I. (2005). Spatial Memory in the Rat Requires the Dorsolateral Band of the Entorhinal Cortex. Neuron *45*, 301–313.

Strozyk, D., Blennow, K., White, L.R., and Launer, L.J. (2003). CSF Abeta 42 levels correlate with amyloid-neuropathology in a population-based autopsy study. Neurology *60*, 652–656.

Supekar, K., Menon, V., Rubin, D., Musen, M., and Greicius, M.D. (2008). Network Analysis of Intrinsic Functional Brain Connectivity in Alzheimer's Disease. PLOS Comput. Biol. *4*, e1000100.

Suzuki, W.A., and Amaral, D.G. (1994). Perirhinal and parahippocampal cortices of the macaque monkey: cortical afferents. J. Comp. Neurol. *350*, 497–533.

Tang, M.X., Cross, P., Andrews, H., Jacobs, D.M., Small, S., Bell, K., Merchant, C., Lantigua, R., Costa, R., Stern, Y., et al. (2001). Incidence of AD in African-Americans, Caribbean Hispanics, and Caucasians in northern Manhattan. Neurology *56*, 49–56.

Tapiola, T., Alafuzoff, I., Herukka, S.-K., Parkkinen, L., Hartikainen, P., Soininen, H., and Pirttilä, T. (2009). Cerebrospinal fluid {beta}-amyloid 42 and tau proteins as biomarkers of Alzheimer-type pathologic changes in the brain. Arch. Neurol. *66*, 382–389.

Toledo, J.B., Bjerke, M., Da, X., Landau, S.M., Foster, N.L., Jagust, W., Jack, C., Jr, Weiner, M., Davatzikos, C., Shaw, L.M., et al. (2015). Nonlinear Association Between Cerebrospinal Fluid and Florbetapir F-18 β-Amyloid Measures Across the Spectrum of Alzheimer Disease. JAMA Neurol. *72*, 571–581.

Treves, A., and Rolls, E.T. (1994). Computational analysis of the role of the hippocampus in memory. Hippocampus *4*, 374–391.

Tsao, A., Moser, M.-B., and Moser, E.I. (2013). Traces of experience in the lateral entorhinal cortex. Curr. Biol. CB *23*, 399–405.

Tsao, A., Sugar, J., Lu, L., Wang, C., Knierim, J.J., Moser, M.-B., and Moser, E.I. (2018). Integrating time from experience in the lateral entorhinal cortex. Nature *561*, 57–62.

US Census Bureau (2020). Racial and Ethnic Diversity in the United States: 2010 Census and 2020 Census.

Vakil, E., and Blachstein, H. (1997). Rey AVLT: Developmental norms for adults and the sensitivity of different memory measures to age. Clin. Neuropsychol. *11*, 356–369.

Van Cauter, T., Camon, J., Alvernhe, A., Elduayen, C., Sargolini, F., and Save, E. (2013). Distinct roles of medial and lateral entorhinal cortex in spatial cognition. Cereb. Cortex N. Y. N 1991 *23*, 451–459.

Vannini, P., Hedden, T., Becker, J.A., Sullivan, C., Putcha, D., Rentz, D., Johnson, K.A., and Sperling, Reisa.A. (2012). Age and amyloid-related alterations in default network habituation to stimulus repetition. Neurobiol. Aging *33*, 1237–1252.

Vemuri, P., Lowe, V.J., Knopman, D.S., Senjem, M.L., Kemp, B.J., Schwarz, C.G., Przybelski, S.A., Machulda, M.M., Petersen, R.C., and Jack, C.R. (2017). Tau-PET uptake: Regional variation in average SUVR and impact of amyloid deposition. Alzheimers Dement. Amst. Neth. *6*, 21–30.

Villemagne, V.L., Fodero-Tavoletti, M.T., Masters, C.L., and Rowe, C.C. (2015). Tau imaging: early progress and future directions. Lancet Neurol. *14*, 114–124.

Vossel, K., Ranasinghe, K.G., Beagle, A.J., La, A., Ah Pook, K., Castro, M., Mizuiri, D., Honma, S.M., Venkateswaran, N., Koestler, M., et al. (2021). Effect of Levetiracetam on Cognition in Patients With Alzheimer Disease With and Without Epileptiform Activity: A Randomized Clinical Trial. JAMA Neurol.

Wagner, G., Gussew, A., Köhler, S., de la Cruz, F., Smesny, S., Reichenbach, J.R., and Bär, K.-J. (2016). Resting state functional connectivity of the hippocampus along the anterior–posterior axis and its association with glutamatergic metabolism. Cortex *81*, 104–117.

Wang, C., Chen, X., Lee, H., Deshmukh, S.S., Yoganarasimha, D., Savelli, F., and Knierim, J.J. (2018). Egocentric coding of external items in the lateral entorhinal cortex. Science *362*, 945–949.

Weintraub, S., Besser, L., Dodge, H.H., Teylan, M., Ferris, S., Goldstein, F.C., Giordani, B., Kramer, J., Loewenstein, D., Marson, D., et al. (2018). Version 3 of the Alzheimer Disease

Centers' Neuropsychological Test Battery in the Uniform Data Set (UDS). Alzheimer Dis. Assoc. Disord. *32*, 10–17.

Weschler, D. (1987). Weschler memory scale-Revised. San Antonio Psychol. Corp.

Willemse, E.A.J., Tijms, B.M., van Berckel, B.N.M., Le Bastard, N., van der Flier, W.M., Scheltens, P., and Teunissen, C.E. (2021). Comparing CSF amyloid-beta biomarker ratios for two automated immunoassays, Elecsys and Lumipulse, with amyloid PET status. Alzheimers Dement. Diagn. Assess. Dis. Monit. *13*, e12182.

Wilson, D.I.G., Langston, R.F., Schlesiger, M.I., Wagner, M., Watanabe, S., and Ainge, J.A. (2013a). Lateral entorhinal cortex is critical for novel object-context recognition. Hippocampus *23*, 352–366.

Wilson, D.I.G., Watanabe, S., Milner, H., and Ainge, J.A. (2013b). Lateral entorhinal cortex is necessary for associative but not nonassociative recognition memory. Hippocampus *23*, 1280–1290.

Wilson, I.A., Gallagher, M., Eichenbaum, H., and Tanila, H. (2006). Neurocognitive aging: prior memories hinder new hippocampal encoding. Trends Neurosci. *29*, 662–670.

Witter, M.P., Doan, T.P., Jacobsen, B., Nilssen, E.S., and Ohara, S. (2017). Architecture of the Entorhinal Cortex A Review of Entorhinal Anatomy in Rodents with Some Comparative Notes. Front. Syst. Neurosci. *11*, 46.

Xia, C.-F., Arteaga, J., Chen, G., Gangadharmath, U., Gomez, L.F., Kasi, D., Lam, C., Liang, Q., Liu, C., Mocharla, V.P., et al. (2013). [18F]T807, a novel tau positron emission tomography imaging agent for Alzheimer's disease. Alzheimers Dement. *9*, 666–676.

Yassa, M.A., and Stark, C.E.L. (2011). Pattern separation in the hippocampus. Trends Neurosci. *34*, 515–525.

Yassa, M.A., Stark, S.M., Bakker, A., Albert, M.S., Gallagher, M., and Stark, C.E.L. (2010). High-resolution structural and functional MRI of hippocampal CA3 and dentate gyrus in patients with amnestic Mild Cognitive Impairment. NeuroImage *51*, 1242–1252.

Yassa, M.A., Mattfeld, A.T., Stark, S.M., and Stark, C.E.L. (2011a). Age-related memory deficits linked to circuit-specific disruptions in the hippocampus. Proc. Natl. Acad. Sci. U. S. A. *108*, 8873–8878.

Yassa, M.A., Lacy, J.W., Stark, S.M., Albert, M.S., Gallagher, M., and Stark, C.E.L. (2011b). Pattern separation deficits associated with increased hippocampal CA3 and dentate gyrus activity in nondemented older adults. Hippocampus *21*, 968–979.

Yeung, L.-K., Hale, C., Last, B.S., Andrews, H., Sloan, R.P., Honig, L.S., Small, S.A., and Brickman, A.M. (2019). Cerebrospinal fluid amyloid levels are associated with delayed memory retention in cognitively normal biomarker-negative older adults. Neurobiol. Aging *84*, 90–97.

Yonelinas, A.P., and Ritchey, M. (2015). The slow forgetting of emotional episodic memories: An emotional binding account. Trends Cogn. Sci. *19*, 259–267.

Yushkevich, P.A., Amaral, R.S.C., Augustinack, J.C., Bender, A.R., Bernstein, J.D., Boccardi, M., Bocchetta, M., Burggren, A.C., Carr, V.A., Chakravarty, M.M., et al. (2015). Quantitative comparison of 21 protocols for labeling hippocampal subfields and parahippocampal subregions in in vivo MRI: Towards a harmonized segmentation protocol. NeuroImage *111*, 526–541.

Zhang, Z., Lu, G., Zhong, Y., Tan, Q., Liao, W., Wang, Z., Wang, Z., Li, K., Chen, H., and Liu, Y. (2010). Altered spontaneous neuronal activity of the default-mode network in mesial temporal lobe epilepsy. Brain Res. *1323*, 152–160.

(2020). 2020 Alzheimer's disease facts and figures.

APPENDIX A

CSF biomarkers of Alzheimer's pathology are highly concordant with amyloid-PET in cognitively normal older adults

Introduction

The presence of protein aggregates comprising of amyloid-β (Aβ; i.e. amyloid plaques) and hyperphosphorylated tau (i.e. neurofibrillary tangles) are hallmark features of Alzheimer's disease (AD) (Blennow et al., 2010; Jack et al., 2018; McKhann et al., 2011; Strozyk et al., 2003). Abnormal accumulation of Aβ and tau proteins in the brain begins 10–20 years before clinical symptom onset (Jack Jr et al., 2010), making biomarkers of these proteins key components of research criteria for preclinical AD and critical for inclusion criteria and outcome measures of clinical trials (Bateman et al., 2012; Dubois et al., 2014; Hof et al., 1996; Perl, 2010).

Currently, the predominant and best-established modalities for assessing Aβ and tau pathologies *in vivo* are measuring concentrations within cerebrospinal fluid (CSF) and visualizing deposition with positron emission tomography (PET). While PET has the advantage of providing information about not only the quantity but the spatial distribution of these proteins, CSF can be more easily acquired and therefore may have more utility for early detection of pathology. However, validating CSF measures against gold-standard PET is critical to fully understanding their utility due to variations in collection and processing methods across studies.

Recent advances in automated assays to quantify AD biomarkers within CSF overcome this variation due to a consistent analytical process. Recent studies comparing the automated

Fujirebio Lumipulse assay with the more widely used INNOTEST ELISAs have shown good concordance between the two platforms, with the Lumipulse demonstrating reduced intra- and inter-assay variability (Bayart et al., 2019). While few studies have assessed the agreement of amyloid-PET and CSF biomarkers on the Lumipulse assay, they have consistently shown that both ratios of Aβ pathology (i.e. Aβ42/40) and overall Alzheimer's pathology (i.e. ptau/Aβ42) have high agreement with amyloid-PET in classifying amyloid-positivity (Alcolea et al., 2019; Campbell et al., 2021; Willemse et al., 2021). However, participants in these studies have mostly been clinical or mixed memory cohorts, with a limited number of cognitively normal participants, which makes the utility of the Lumipulse assay and its published thresholds for amyloid-positivity in preclinical samples undetermined, although critical for research on the development of AD.

In the current study, we validate CSF AD biomarkers derived from the Lumipulse assay against amyloid-PET in an entirely cognitively normal sample. We examined the CSF biomarkers of $A\beta_{1\text{-}40}$, $A\beta_{1\text{-}42}$, phospho-tau (p-tau_{181}), total tau (t-tau), as well as the Aβ42/40 and p-tau/Aβ42 ratios, to test a range of pathological markers against the widely used ^{18}F-Florbetapir PET. In this cognitively normal sample, our aims were to (1) determine the strength of continuous associations between CSF biomarkers and levels of amyloid-PET, (2) test the concordance of previously published thresholds for "positive" CSF biomarkers (i.e. Aβ42/40 and ptau/Aβ42) derived from a predominantly clinical sample (Alcolea et al. 2019) with Aβ -PET positivity; and (3) determine which CSF biomarkers are most predictive of Aβ-PET classification.

Participants

Thirty-two (N = 32) cognitively normal (Clinical Dementia Rating [CDR] = 0) older adults between 64 and 86 years of age (24 F, mean = 73.5 years, SD = 4.72 years) were recruited from the Alzheimer's Disease Research Center (ADRC) Longitudinal Cohort at the University of California, Irvine. Demographic information about the participants is displayed in **Table A1**. Participants gave written informed consent in accordance with the Institutional Review Board of the University of California, Irvine, and were compensated for their participation.

Demographics	
Sample Size	32
Age (years)	73.5 (4.72)
Sex	24F (75%)
Education (years)	16.4 (2.42)
MMSE (points)	28.2 (1.59)
APOE Status	
e4 +	12 (38.7%)
e4 -	19 (61.3%)
Missing	1
Aβ42 (pg/mL)	616 (298)
t-tau (pg/mL)	307 (128.00)
p-tau (pg/mL)	42.4 (20.10)
Aβ42/40	0.069 (0.23)
p-tau/Aβ42	0.098 (0.11)
FBP Mean SUVR	1.14 (0.18)
Time between CSF-PET (years)	0.92 (0.82)

Table A1. Demographics and summary measures of the cognitively normal older adult cohort. Data represents mean (standard deviation) or N (%). MMSE, Mini Mental State Exam; APOE, Apolipoprotein E; t-tau, total tau; p-tau, phosphorylated tau_{181}; FBP, ^{18}F-Florbetapir PET; SUVR, standardized uptake value ratio.

CSF Acquisition and Processing

Cerebrospinal fluid (CSF) was obtained from participants via lumbar puncture, performed with standard clinical research methods in aseptic fashion by a board-certified neurologist. The CSF was collected in a 15mL Falcon tube, placed on ice until processed (within 2 hours), aliquoted into 250 microliter volumes and stored at -80 degrees Celsius until use. CSF was always collected during a separate session from PET imaging visit with an average time interval of 0.96 years.

$A\beta_{1-42}$, $A\beta_{1-40}$, phosphorylated tau_{181} (p-tau), and total tau (t-tau) were quantified in human CSF on the Lumipulse *G* 1200 automated platform using a chemiluminescent enzyme immunoassay (CLEIA) by the UCSD Shirley-Marcos ADRC Biomarker Core.

PET Acquisition and Processing

All participants in the current study received positron emission tomography (PET) with the ^{18}F-Florbetapir (FBP) tracer to quantify Aβ. PET was performed on an ECAT high Resolution Research Tomograph (HRRT, CTI/Siemens, Knoxville, TN, USA). Ten mCi of tracer was injected, and four five-minute PET scan frames were collected from 50-70 min post-injection. Reconstruction was performed using 3D ordinary Poisson ordered subset expectation maximization with attenuation correction, and 4mm Gaussian smoothing. SUVR images were coregistered to the T1 image and normalized by a whole cerebellum reference region. Additional smoothing using a 6mm Gaussian kernel was then applied to achieve an effective resolution of

8mm^3. The mean SUVR of a previously validated cortical composite region (FreeSurfer ROIs including frontal, cingulate, parietal, and temporal regions; see (Alcolea et al., 2019; Campbell et al., 2021; Willemse et al., 2021) was quantified, and used to determine FBP positivity using a threshold of >1.11 SUVR.

Structural MRI

All participants received a structural MRI on a 3T Prisma scanner (Siemens Medical System) with a 32-channel head coil. A whole-brain high resolution T1-weighted volumetric magnetization prepared rapid gradient echo image (MPRAGE) was acquired (TR/TE/TI = 2300/2.38/902 ms, flip angle = 8°, resolution = 0.8mm isotropic, 240 slices acquired sagittally). Structural MRIs were used for PET coregistration and were processed through FreeSurfer v.6.0 to obtain native-space regions of interest for FBP quantification.

Statistical Analysis

Bivariate correlations were used to examine the relationship between CSF biomarkers and FBP mean SUVR, covarying for the time between PET and CSF acquisition. Correlation plots were generated using GraphPad Prism (v.9.2.0).

Receiver operator characteristics (ROC) were performed using random forest models with Aβ-PET status as the outcome and CSF biomarkers status as predictors. CSF cutoffs were based on Alcolea et al. (2019), with a cutoff of 0.062 for Aβ42/40, and 0.068 for p-tau/Aβ42 (Alcolea et al., 2019). We compared false positive rate with true positive rate to generate the area under the ROC curve (AUC) for each ratio.

We investigated the most relevant features associated with Aβ-PET positivity using random forest feature selection importance rates. The Gini impurity importance indicates how

often a particular feature was selected for a split, and how large its overall discriminative value was to the classification. The top importance features are the ones whose Gini node purity is higher, because its absence shows the largest change in the prediction.

We used cutpointr, a statistical software for the selection of optimal cutoffs implemented in R statistical software (version 3.6.3). CSF measures were compared to Aβ-PET positivity with ROC, and cutoffs showing the highest Youden index were selected. We then compared specificity with sensitivity to generate the area under the ROC curve (AUC) for each ratio.

Demographics

A total of 32 participants received both CSF and PET measures of Aβ and were included in the present analysis. Full demographic information of the sample is presented in **Table A1.** Participants were an average age of 73.5 years old, were predominantly female (75%), and received CSF and PET measurements within an average of 0.92 years. One participant had 5.75 years between CSF and PET (classified as positive on both measurements) – all analysis were conducted with and without this participant, although results remained consistent regardless of inclusion. One participant's p-tau and t-tau levels were a significant outlier (>2 SD of sample mean); this this data point was removed from analyses involving these measures.

Associations between CSF and PET Measures

First, we examined the relationship between mean FBP SUVR and CSF measures of AD pathology in our cognitively normal sample. There was a significant correlation between FBP SUVR and both Aβ42 ($r = -0.728$, $p<0.001$; **Fig A1A**) and p-tau ($r=0.40$, $p=0.034$; **Fig A1B**), but not t-tau ($r = 0.24$, $p = 0.86$; **Fig A1C**). Additionally, mean FBP SUVR was associated with the Aβ42/40 ratio ($r = -0.81$, $p<0.001$; **Fig A1D**), indicating that FBP has a strong relationship with

AD-specific Aβ pathology. Finally, there was a strong association between FBP and p-tau/Aβ42, a ratio representing total levels of AD-related pathology, which was strongest when using a curvilinear model (curvilinear fit: ρ=0.84, p<0.001; linear fit: r = 0.65; p<0.001; **Fig A1E**). All associations remained significant and of similar correlational values when removing the one participant with 5.75 years between PET and CSF.

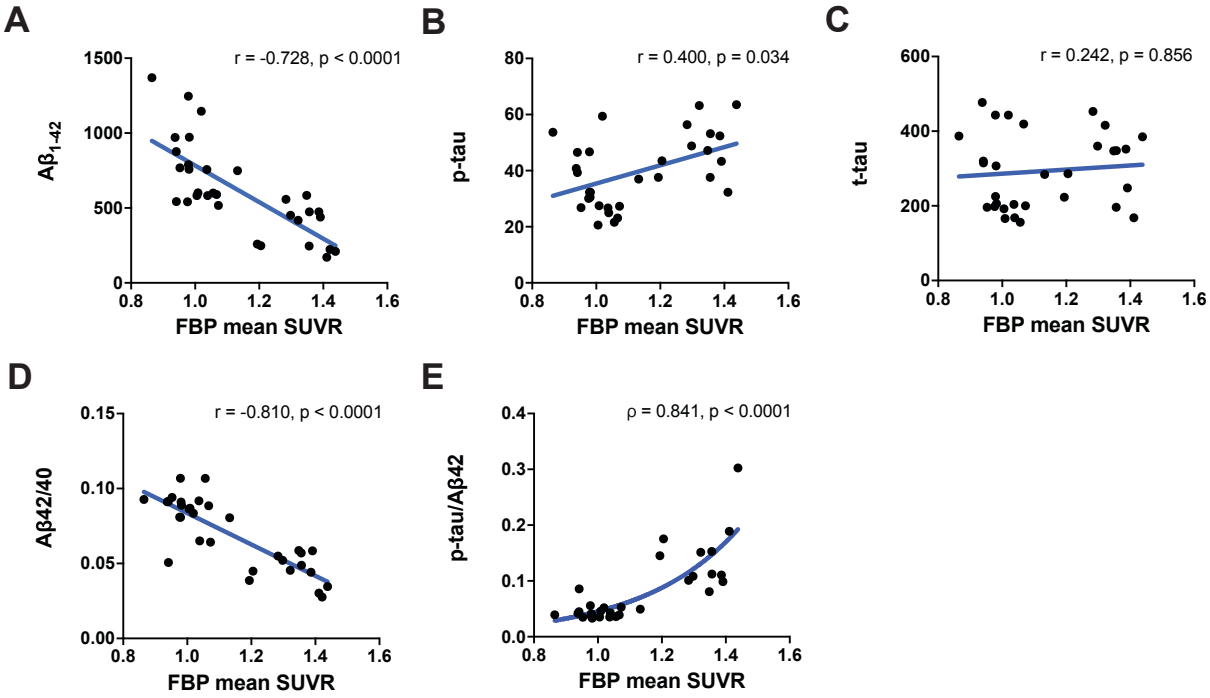

Figure A1. CSF biomarkers are highly correlated with Aβ-PET in cognitively normal older adults. Increased ^{18}F-Florbetapir (FBP) mean SUVR was significantly correlated with decreased CSF $A\beta_{1\text{-}42}$, indicating more Aβ (A) and increased p-tau, indicating more phosphorylated $tau_{181;}$ B). There was no association between FBP Mean SUVR and total tau (t-tau) (C). FBP mean SUVR was also significantly associated with decreased Aβ42/40 ratio, indicating more Aβ specific to Alzheimer's disease (D), and increased p-tau/Aβ42, indicating more overall Alzheimer's pathology (E).

Concordance between CSF and PET Aβ Positivity

We next determined whether participants classified as Aβ+ on PET using a validated threshold (>1.11 SUVR; (Landau et al., 2012) would also be considered positive for CSF Aβ42/40 using a threshold calculated in a mixed memory cohort (<0.062; (Alcolea et al., 2019).

The majority of subjects were concordant on the two measures (30/32, 93.8%; **Fig A2A**). Thirteen participants were classified concordant positive (40.5%), 17 participants as concordant negative (53.1%), and one participant was classified into each of the discordant groups.

To determine the classification performance of CSF Aβ42/40 positivity compared to Aβ-PET positivity, we next conducted random forest ROC analyses. CSF Aβ42/40 status predicted Aβ-PET status with high accuracy (0.93 ± 0.13) and precision (0.93 ± 0.17), with an AUC value of 0.92 ± 0.16 (**Fig A2B**). Results were consistent when using logistic regression models to ensure the random forest model did not overfit the data.

We next tested whether Aβ-positivity on PET was also consistent with a positive p-tau/Aβ42 ratio (>0.068, Alcolea et al 2019). Consistent with Aβ42/40, the majority of subjects were concordant between p-tau/Aβ42 and Aβ-PET (30/32, 93.8%; **Fig A2C**), with 13 participants were classified concordant positive (40.5%), 17 participants as concordant negative (53.1%), and one participant was classified into each of the discordant groups. Random forest ROC analyses showed that classification performance of p-tau/Aβ42 status had high accuracy (0.93 ± 0.13) and precision (0.97 ± 0.17) when compared to Aβ-PET status, with an AUC value of 0.95 ± 0.10 (**Fig A2D**).

Finally, we conducted a Gini impurity analysis to test which CSF biomarkers were most important in predicting Aβ-PET status, when also including age and PET-CSF interval (**Fig A2E**). We measured the importance of each feature with the Gini impurity importance, and these measures highlight p-tau/Aβ42 as the most relevant features for Aβ-positivity, followed by Aβ42/40. The ranking indicated that the least influential features of the predictions are age, t-tau, and PET-CSF interval.

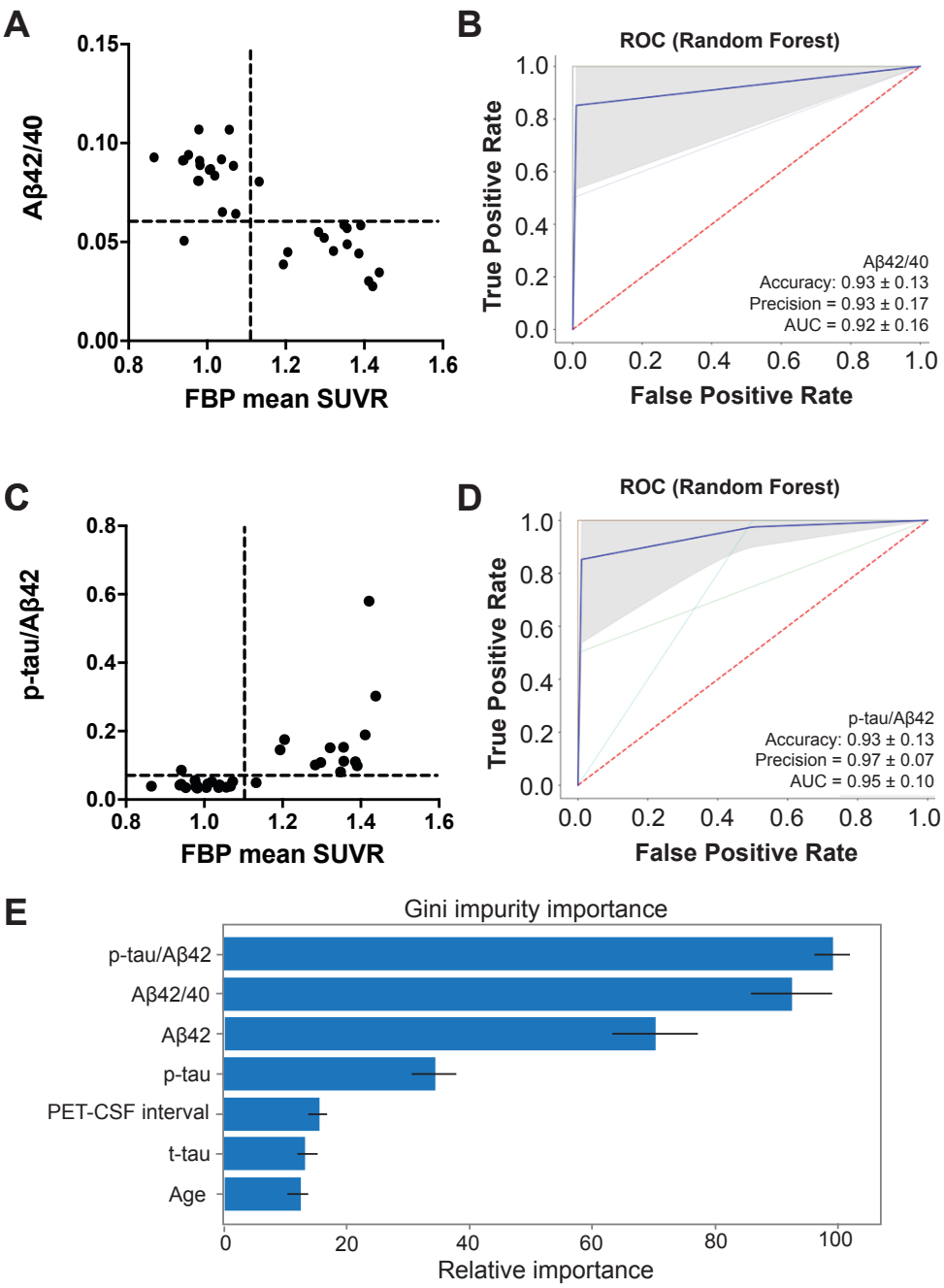

Figure A2. Positivity on Aβ-PET and CSF biomarkers are highly concordant in cognitively normal older adults. (A, C) Concordance for Aβ-PET and both CSF Aβ42/40 (A) and p-tau/Aβ42 (C) was 93.8% (13 concordant positive, 17 concordant negative, 2 discordant). (B, D) Random Forest ROC analyses indicated that both CSF Aβ42/40 (B) and p-tau/Aβ42 (D) predicted Aβ-PET status with high accuracy. (E) Gini impurity analysis indicated that CSF p-tau/Aβ42 was the more important feature in predicting Aβ-PET status, with nearly 100% relative importance. The bars represent the importance of each feature (error bars represent standard deviation), measured through the sum of all the Gini impurity index decreases for each specific feature.

Replication of Data-driven CSF Thresholds

Finally, we recalculated data-driven thresholds for CSF biomarkers that were optimal for our cognitively normal sample. CSF measures were compared to Aβ-PET positivity, and cutoffs showing the highest Youden index were selected. The optimal Aβ42/40 cutoff was 0.059 (Youden index of 0.873; **FigA3A**), which predicted Aβ-PET status with high accuracy (0.937) and precision (1.00), with an AUC value of 0.97 (**FigA3B**). The optimal p-tau/Aβ42 cutoff was 0.081 (Youden index of 0.928; **FigA3C**), which predicted Aβ-PET status with high accuracy (0.969) and precision (1.00), with an AUC value of 0.98 (**FigA3D**).

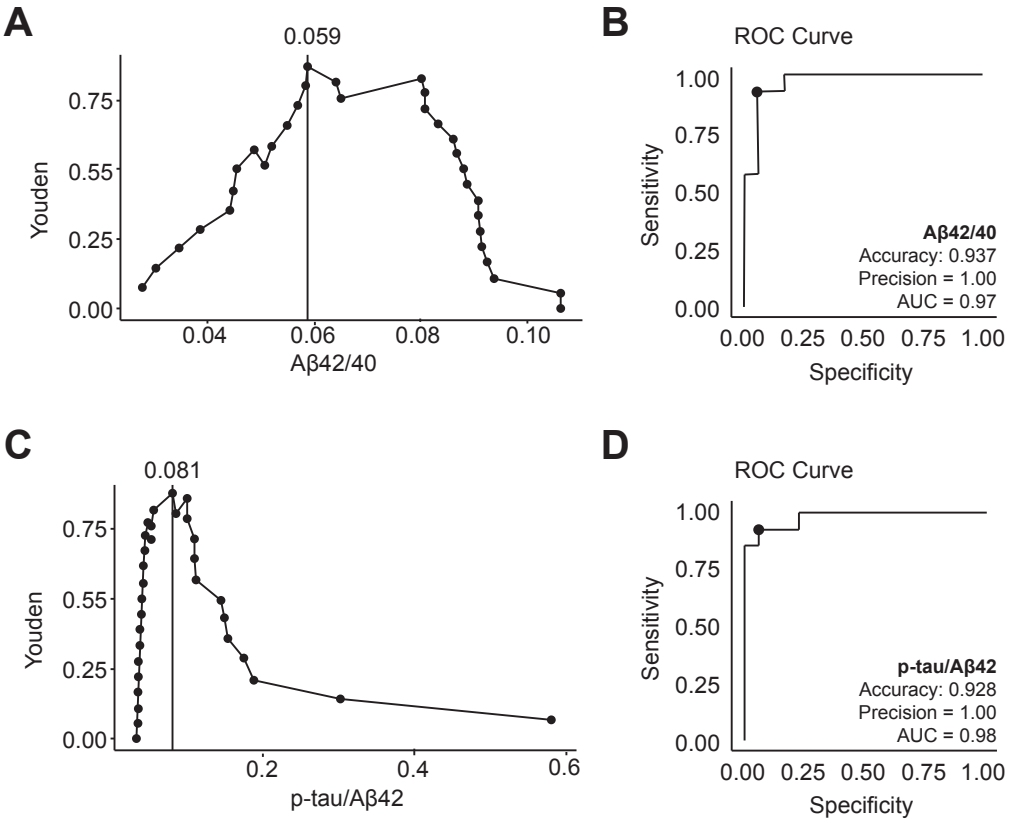

Figure A3. Recalculation of thresholds for CSF Aβ42/40 and p-tau/A42 in a cognitively normal sample. (A) The optimal threshold for Aβ42/40 was determined to be 0.059, representing the highest Youden index (0.929). (B) Using the 0.059 cut-off, CSF Aβ42/40 status predicted Aβ-PET status with high accuracy and precision. C) The optimal threshold for p-tau/Aβ42 was determined to be 0.081, representing the highest Youden index (0.928). (B) Using the 0.081 cut-off, CSF p-tau/Aβ42 status predicted Aβ-PET status with high accuracy and precision.

Discussion

Our findings support a strong association between CSF biomarkers of AD derived using an automated Lumipulse assay with Aβ-PET for the first time in an entirely cognitively unimpaired sample. Aβ-PET and CSF biomarkers of Aβ (Aβ42/40 and $A\beta_{1\text{-}42}$), p-tau, and p-tau/Aβ42 were strongly correlated, which is consistent with previous findings in mixed memory cohorts (Alcolea et al., 2019; Campbell et al., 2021; Willemse et al., 2021). We demonstrated that CSF Aβ42/40 and Aβ-PET positivity are highly concordant in cognitively normal older adults using a threshold previously calculated in a mixed-memory cohort. Further, CSF p-tau/Aβ42, a marker of overall AD pathology, was the strongest predictor of Aβ-PET. Together, our results support the accuracy of the automated Lumipulse assay to quantify CSF biomarkers of AD in cognitively normal samples, and the utility of these biomarkers in measuring emerging AD pathology in aging.

Our results expand on previous studies investigating CSF biomarker relationships with Aβ-PET in mixed memory or clinical cohorts (Campbell et al., 2021). A previous study in a mixed memory cohort reported that Aβ42/40 and p-tau/Aβ42 ratios were equally predictive of Aβ-PET status (Campbell et al., 2021). In our sample, while classification agreement and performance were similar between CSF Aβ42/40 and p-tau/Aβ42 in predicting Aβ-PET positivity, p-tau/Aβ42 demonstrated slightly higher precision than Aβ42/40, resulting in a higher

AUC value. Furthermore, p-tau/Aβ42 was the most important feature selected in predicting Aβ-positivity, followed by Aβ42/40. These findings indicate that the p-tau/Aβ42 ratio may be more sensitive in a cognitively normal sample, as it also accounts for the amount of phosphorylated tau pathology, and may more accurately represent overall AD pathology.

Recalculating data-driven CSF Aβ42/40 and p-tau/Aβ42 thresholds on our own dataset of cognitively normal older adults, we derived a very similar threshold to Alcolea et al. (Alcolea et al., 2019). However, our thresholds are slightly lower for Aβ42/40 (0.059) and higher for p-tau/Aβ42 (0.081) in our cognitively normal sample compared to the cutoff reported in Alcolea et al. (0.061 for Aβ42/40 and 0.068 for p-tau/Aβ42) in their mixed memory cohort. This difference may be due to our use of a quantitative threshold for defining Aβ-PET positivity, while Alcolea et al. used visual reads. Further, our thresholds may more accurately measure emerging AD pathology, as they were derived without the influence of measures from clinically impaired subjects.

Limitations of the current study include the relatively small sample size, and the variation of time between CSF and PET measurements, however, this was controlled for in all analyses. We could not characterize why PET and CSF measures were discordant in our study due to the limited in the number of discordant observations (2 participants). Future research should investigate the longitudinal changes that occur in concordant individuals compared to those that are discordant, and determine whether CSF may be more sensitive and changes prior to PET in preclinical samples.

Overall, our findings support the utility of quantifying CSF biomarkers with the automated Lumipulse assay in studies of cognitively normal participants, and emphasize the

importance of CSF biomarkers to measure emerging AD pathology in cognitively normal samples.